Analysis and design of offshore tubular members against ship impacts

Zhaolong Yu [a, b*], Jørgen Amdahl [a, b]

a, Department of Marine Technology, Norwegian University of Science and Technology (NTNU), Norway

b, Center for Autonomous Marine Operations and Systems (AMOS), Norwegian University of Science and Technology (NTNU), Norway

Abstract

Ship collisions may be critical to the operational safety of ships and offshore structures, and should be carefully designed against. This paper investigates the response of offshore tubular members subjected to vessel bow and stern impacts with the nonlinear finite element code LS-DYNA. Two 7500 tons displacement supply vessels of modern design are modeled. Force-displacement curves for bow and stern indentation by rigid tubes are compared with design curves in the DNV-GL RP C204. Next, both the ship structure and the tubular braces/legs are modelled using nonlinear shell finite elements, and the effect of ship-platform interaction on the damage distribution is investigated. A parametric study of the denting mechanics with respect to the length, diameter and wall thickness of tubular members is described. An existing analytical denting model is extended to account for distributed loads and is verified against simulation results. Existing requirements to resist excessive local denting are discussed, and a new concept 'transition indentation ratio' is introduced. The concept helps to understand the governing deformation patterns of tubular members given different tube dimensions, and is useful to unify existing cross section compactness criteria for braces/legs, providing a theoretical support for the R_c criterion in the new version DNV-GL RP C204 standard. Finally, new design compactness requirements for tubular members against impacts from ship bow, stern corner and stern end are proposed.

Key words: ship collisions; tubular braces/legs; damage assessment; denting mechanics; transition indentation ratio;

1. Introduction

The current DNV-GL RP C204 standard for the design of ships and offshore structures against accidental ship collisions were developed decades ago [1]. Many procedures were based on simplified plastic methods, and some of the requirements seem to be outdated now. A noticeable example is that a significant increase of the design impact energy may be needed according to Kvitrud [2], who summarized collision accidents in Norway in the period 2001-2010. Recently, a new version of the DNV-GL RP C204 standard for ship impacts is under preparation in DNV-GL, and the NORSOK N004 appendix A code [3] may be revised as well in the near future. The purpose of this work is to provide useful suggestions for improvements of the new standard. This will be done through simulations of tubular braces/legs impacted by a ship bow and two ship sterns using the nonlinear finite element code LS-DYNA.

In the design of offshore structures against accidental loads, significant damage can be allowed provided that the damage shall not impair the main safety functions such as the global load bearing capacity of structures and the usability of escape ways. The energy to be dissipated in

* Corresponding author, Dr. Zhaolong Yu Email: zhaolong.yu@ntnu.no

ship collisions can vary with different displacements and velocities of the striking vessel. Based on risk analysis, the present DNV-GL RP C204 standard [4] suggests a standard vessel with a displacement of 5000 tons travelling with a speed of 2m/s. This gives a kinetic energy of 11 MJ for bow/stern impacts and 14 MJ for broad side impacts considering the hydrodynamic effects with simple added masses. More considerations regarding the hydrodynamic effects during ship collisions can be found in refs. [5-7]. The recommended deformation resistance curves for side, bow and stern impacts are given in Fig. 1. However, with the sizes of supply vessels increasing significantly to 7500-10000 tons and the impact speed higher than 2 m/s as identified in Kvitrud [2], the current design energy is considered too low. In addition, the validity of the current design curves can be questioned by the modern design of ship structures and advanced simulation tools.

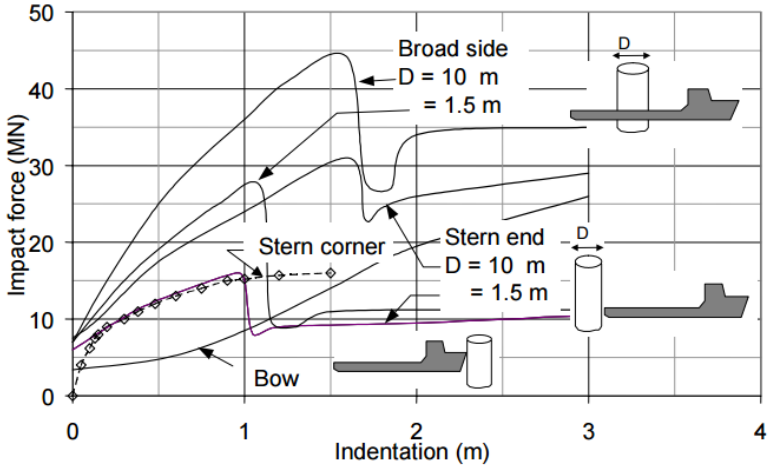

Fig. 1. Recommended force-displacement curve for beam, bow and stern impacts [3]

As concerns the impact responses of tubular members in offshore structures like jack-ups and jacket platforms, an idealized model for the deformation may be described as follows: the tubular brace/leg deforms firstly with local denting and absorbs energy. At the same time, the plastic bending capacity of the dented brace is reduced due to the detrimental effect on the section modulus. When a certain indentation is reached, the brace starts to collapse as a beam via a three-hinge mechanism. Upon further crushing of the brace, axial membrane forces will occur and get dominant up to fracture if adjacent structures are capable of providing sufficient strength against the pull-in. Local denting may either cease or continue in the beam deformation stage.

The governing parameters for the impact response of a brace/leg are quite a few such as tube length, diameter, thickness, material properties, contact width, restraint conditions at tube ends, axial preloading, striker geometry, impact locations, etc. The high number of parameters makes the deformation mechanics of tubular members complicated. Extensive studies have been carried out to understand the underlying mechanics by means of experiments, numerical simulations and theoretical derivations. A few theoretical models have been proposed and verified through experiments, such as the denting models by Furnes and Amdahl [8], Amdahl [9] and Wierzbicki and Suh [10], the beam bending model by Soares and Søreide [11], and the models containing both denting and bending by Ellinas and Walker [12], Jones and Shen [13] and Buldgen et al. [14]. Experimental data can be found in Amdahl [15], Jones et al. [16] and Sherman [17], etc.

Existing theoretical models and experiments are generally based on the idealized scenario that a rigid indenter with a certain shape (typically wedge-shaped or rectangular) strikes into a tube with clamped ends. However, ship collision situations may include various striking geometries, contact widths and boundary conditions. The problem can be even more complicated considering the relative strength between the struck brace/leg and the striking ship. It can be questioned whether the theoretical models can be applied in real ship collision analysis and crashworthiness design, and second, how accurate are they.

With respect to the distribution of strain energy, three categories are often assumed: strength design, ductile design and shared-energy design. Normal seized jacket braces are not strong enough to resist the ship impact forces, and hence ductile design is often applied for tubular braces where the installations are assumed to dissipate most of the collision energy. As the design collision energy in the new RP increases significantly, a single tubular member cannot absorb the whole collision energy in general. If several tubular members are assumed to absorb the energy, the global integrity of the platform may be threatened and the platform may collapse. A noticeable example is the well workover vessel Big Orange XVIII that collided with the Ekofisk 2/4 jacket platform with a kinetic energy of about 60 MJ, which is far beyond the design energy 11 MJ. The accident causes severe damage to the three legged jackets and also the bow [2], see Fig. 2. Several braces of the jackets are ruptured and the jacket had to be dismantled.

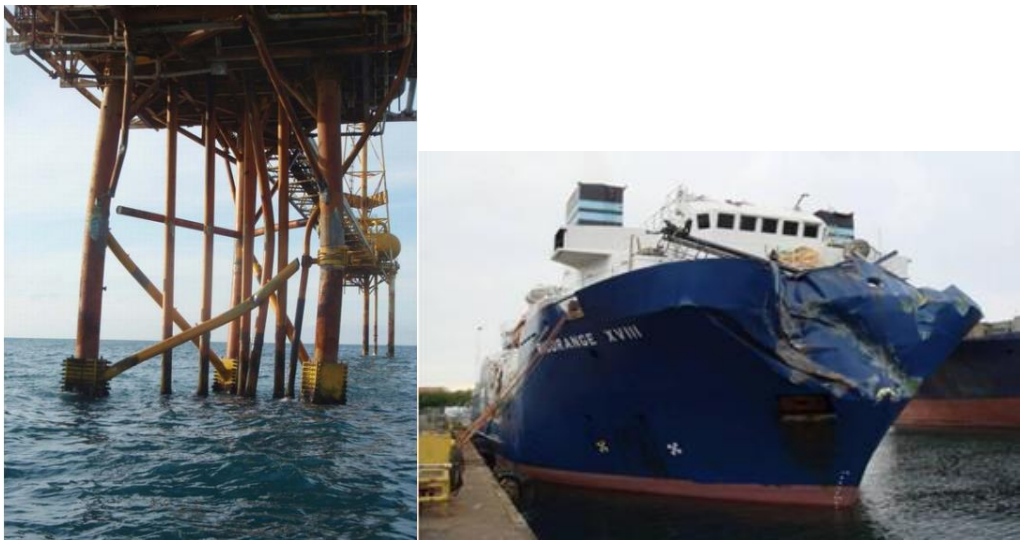

Fig. 2. Big orange-Ekofisk 2-4/W collision

The design energy has increased significantly in the new version NORSOK N003 standard [18]; unless further evaluations are performed, the kinetic energy should be 50 MJ for bow impact, 28 MJ for broad side collisions and 22 MJ for stern collisions. This represents a substantial increase of the demand for collision resistance of an offshore structure. Ductile design may not be appropriate as the braces and legs will otherwise be subjected to very large deformations as shown in studies by Amdahl and Johansen [19], who simulated high energy ship bow-jacket collisions with kinetic energy in the range of 40-50 MJ. It is therefore necessary to go for strength design or shared-energy design for braces/legs, where the ship should deform and dissipate considerable energy. Braces/legs shall not suffer major local denting if the shared-

energy design is assumed. Unfortunately, we can hardly find commonly agreed requirements from the literature and design standards for a brace/leg to maintain compactness during deformation. Existing requirements to resist local denting are generally obtained by observations of either experimental results or numerical simulations. Theoretical supports are lacking.

This paper investigates the behavior of tubular braces/legs subjected to ship collisions accounting for ship-platform interaction. The striking objects include a bulbous bow model and a stern model, both of which are taken from a modern supply vessel with a displacement of 7500 tons. Another realistic stern model of a 7500-ton supply vessel with a different design is also studied. Models of the ship bow and stern ends/corners are first indented by rigid braces. The resulting curves may provide useful indications for the design curves in the new version DNV-GL RP C204 standard. Afterwards, extensive collision simulations with a total energy dissipation of 30-50 MJ are carried out, where both the ship and tubular braces/legs can deform and dissipate energy. The diameter, length and thickness of the tubes are varied. A new concept, 'the transition indentation ratio' from local denting to global bending, is proposed for tube deformation. Design considerations for braces/legs subjected to ship impacts are discussed with respect to denting mechanics and compactness criteria. The findings in this paper will hopefully provide useful suggestions to the new version DNV-GL RP C204 standard.

2. Background

2.1 Theoretical models for denting of tubular braces

Furnes and Amdahl [8] were among the first to study the deformation behavior of tubes under lateral loading. They defined the following relationship between the denting resistance *R* and the depth of penetration w_d:

$$R = 15 \cdot \frac{1}{4}\sigma_y t^2 \sqrt{\left(\frac{D}{t}\right)\left(\frac{2w_d}{D}\right)} \tag{1}$$

where D is the tube diameter, t is the tube wall thickness and σ_y is the yield stress.

Amdahl [9, 15] proposed a local denting model based on plastic yield line analysis, relating the denting resistance to local indentations. This model assumes a flat indenter shape to represent the ship end or side, and the tube is dented with a flattened cross section. A curve that was fitted to these results, is adopted in NORSOK N-004 and plotted in Fig. 3. It has the following form:

$$R/R_c = c_1\left(\frac{w_d}{D}\right)^{c_2} \quad k = \left(22 + 1.2\frac{B}{D}\right)\left(\frac{w_d}{D}\right)^{\frac{1.925}{3.5+\frac{B}{D}}} \cdot \sqrt{\frac{4}{3}\left(1 - \frac{1}{4}\left[1 - \frac{N}{N_p}\right]^3\right)} \tag{2}$$

where B is the contact height. The last term was later borrowed from Wierzbicki and Suh [10] to account for the interaction between denting and axial functional loads in the leg N. N_p is the plastic axial force, and R_c is a characteristic denting resistance of the tube defined as:

$$R_c = \sigma_y \frac{t^2}{4}\sqrt{\frac{D}{t}} \tag{3}$$

Wierzbicki and Suh [10] made the first attempt to develop a closed form solution for the indentation of tubes subjected to lateral concentrated loading under different boundary conditions. They obtained the following force-deflection relationship:

$$R = 16\sqrt{\frac{2\pi}{3}\frac{D}{t}\frac{w_d}{D}}\cdot\frac{1}{4}\sigma_y t^2\sqrt{\left(1-\frac{1}{4}\left[1-\frac{N}{N_p}\right]^3\right)} \tag{4}$$

A big advantage of this expression is that it is derived theoretically, but still preserves a simple form. We have followed Wierzbicki and Suh [10]'s derivation of energy dissipation and extended the model to account for distributed loads with a contact width of *B*. The following equation is obtained:

$$R = 16\left\{\sqrt{\frac{2\pi}{3}\frac{D}{t}\frac{w_d}{D}}\cdot\sqrt{1-\frac{1}{4}\left(1-\frac{N}{N_p}\right)^3}+\frac{B}{D}\right\}\cdot\frac{1}{4}\sigma_y t^2 \tag{5}$$

In the non-dimensional format, it reads:

$$\frac{R}{R_c} = 16\left\{\sqrt{\frac{2\pi}{3}\frac{w_d}{D}}\cdot\sqrt{1-\frac{1}{4}\left(1-\frac{N}{N_p}\right)^3}+\frac{B}{D}\sqrt{\frac{t}{D}}\right\} \tag{6}$$

Ellinas and Walker [12] investigated both local denting and global bending process of tubular members. The tube was assumed to cease deforming locally when global bending started. They proposed the following expression for the denting of tubes:

$$R = K\cdot\frac{1}{4}\sigma_y t^2\sqrt{\frac{w_d}{D}} \tag{7}$$

where, K is a constant coefficient representing the shape of the indenter. It is normally assumed to be 150 for point loading according to experimental observations.

Cho [20] proposed an empirical equation for the denting resistance considering the contact width:

$$\frac{R}{m_0} = 2.0\left(\frac{D}{t}\right)^{0.2}\left(\frac{E}{\sigma_y}\right)^{0.5}\left(\frac{w_d}{D}\right)^{0.45}\exp\left\{0.1\left(B/D\right)\left(\frac{w_d}{D}\right)^{-0.3}\right\} \tag{8}$$

where $m_0 = \frac{1}{4}\sigma_y t^2$.

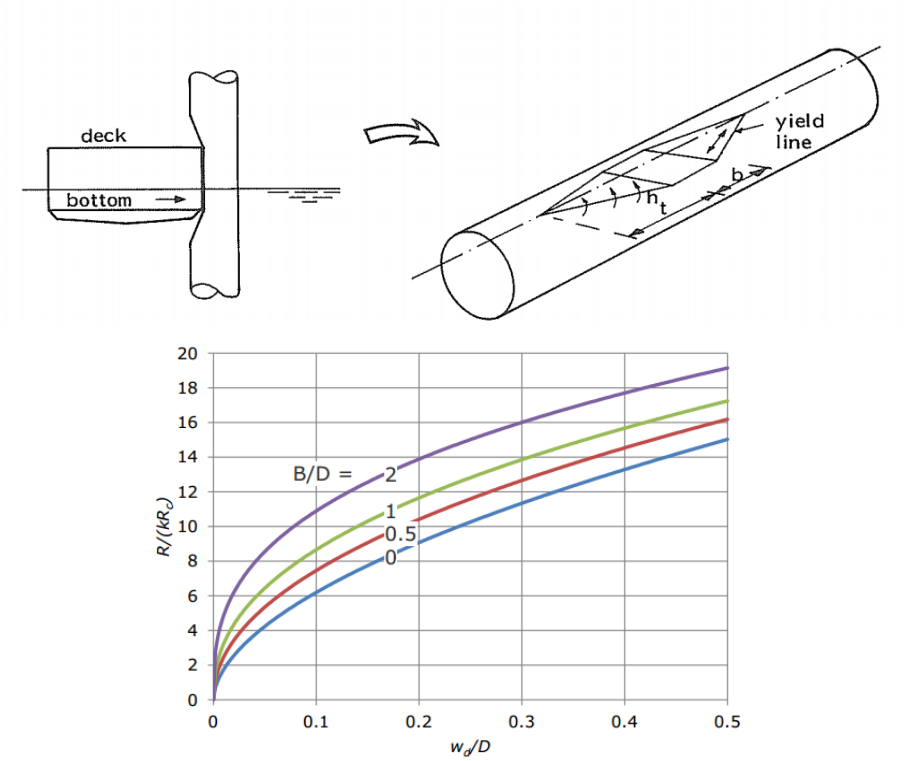

Fig. 3. The resistance curve for local denting, from Amdahl [15]

The reduction in plastic bending moment capacity due to local denting is considered in the DNV-GL RP C204 standard [4] (see Fig. 4). The flat part of the dented cross section is conservatively assumed non-effective, and this yields:

$$\frac{M_{res}}{M_p} = \cos\frac{\theta}{2} - \frac{1}{2}\sin\theta$$
$$M_p = \sigma_y D^2 t \tag{9}$$
$$\theta = \arccos\left(1 - 2\frac{w_d}{D}\right)$$

where M_p and M_{res} are the full and residual plastic bending moment of the tube, respectively.

If the brace is clamped at both ends and is hit at the brace mid-section, the plastic collapse resistance is given by:

$$R_{0,res} = \frac{4M_p}{L}(1+k) \tag{10}$$

where $k = M_{res}/M_p$ is the relative magnitude of the residual and the full plastic bending capacity of the brace. If the brace is not dented, the full plastic bending capacity can be maintained and is $R_0 = 8M_p/L$ by assuming point loads. If the contact is of a certain width, the effective length

should be used by removing the contact width B from the total length L. The effective R_0 increases with reduced effective length.

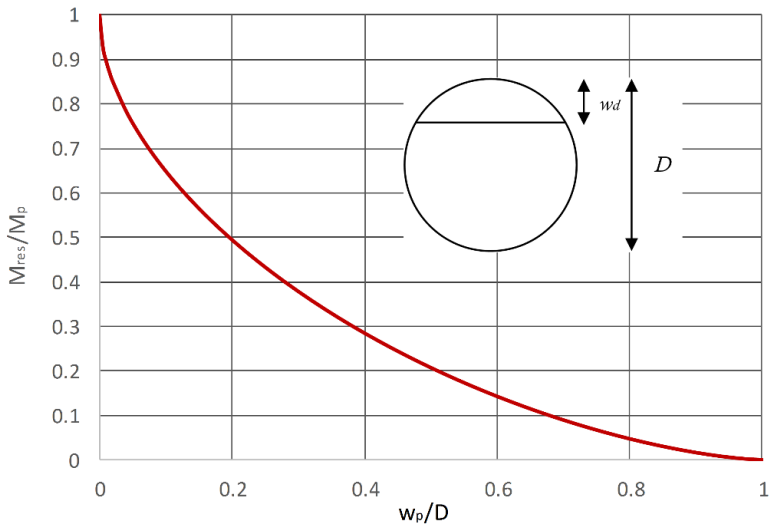

Fig. 4. Reduction of moment capacity due to local dents

2.2 Review of existing criteria to resist local denting

Existing criteria for a brace/leg to remain compact under lateral impacts are generally based on experimental observations and numerical results, but theoretical supports are lacking.

Soares and Søreide [11] presented an analytical solution for the beam deformation of tubular members considering the interaction between bending moment and axial forces. Local denting was assumed to be negligible. Good agreement with numerical simulations was obtained for minor denting. They suggested that members with D/t of 35 or less and L/D up to 22, can be considered to maintain full bending capacity during sustained deformation in accordance with Sherman [17]'s experimental observations.

The API rules [21] prescribe $D/t < 9000/f_y \left(f_y \; in \; Mpa\right)$ to maintain full capacity through plastic deformation. For $9000/f_y < D/t < 15200/f_y$, only a limited plastic rotation capacity can be assumed.

The NORSOK N004 [3] and DNV-GL RP C204 [4] require the following compactness criterion to avoid excessive local denting of the tube before the formation of a three-hinge collapse mechanism:

$$R_0 / R_c < 6 \tag{11}$$

Through observations of numerical simulations, Storheim and Amdahl [22] showed that the criterion was overly conservative. They proposed to use R_c as a characteristic strength factor, and R_c should be larger than 1.7 for bow collisions and 1.3 for vessel side collisions to fulfill the compactness requirements.

Recently, Cerik et al. [23] carried out extensive numerical simulations with ABAQUS and proposed to use the indicator R_0/R_c, to classify the impact responses of tubular members. Four response modes were suggested:

Mode 1: $R_0 / R_c < 6.5$; dominated by global bending

Mode 2: $6.5 \leq R_0 / R_c \leq 1($; dominated by both local denting and beam deformation, and local denting ceases immediately after plastic collapse.

Mode 3: $10 \leq R_0 / R_c \leq 23$; dominated by both local denting and beam deformation, and local denting continues after plastic collapse.

Model 4: $R_0 / R_c > 23$; dominated by local shell denting.

Mode 1 seems to agree with the present DNV-GL RP C204 standard [4].

3. FE modeling of supply vessel bow and sterns

3.1 Material modelling

When the ship-platform interaction shall be accounted for, proper material modelling is essential because the relative strength of the striking and struck objects are very sensitive to material strength and rupture. The power law model was used to model the plastic strain hardening of steel. It includes a yield plateau that delays the onset of hardening. The material properties for the ship and the braces/legs are given in Table 1.

Table 1. Material properties for the ship and brace/leg models

Material	σ_y *(Mpa)*	*E (Gpa)*	*K (Mpa)*	*n*	$\varepsilon_{plateau}$
Ship bow	275	207	830	0.24	0.01
Ship sterns, braces/legs in stern collisions	285	207	740	0.24	0
Braces/legs in bow collisions	420	207	760	0.15	0.005

The Rice-Tracey-Cockcroft-Latham (RTCL) criterion [24] with proper mesh scaling is used to model fracture. The fracture criterion has been proved to be of good accuracy under various loading conditions.

3.2 Finite element models

The numerical simulation was carried out by using the explicit finite element software LS-DYNA 971. The four-node Belytschko-Lin-Tsay shell element was used with reduced integration and 5 integration points through the thickness. It is based on a co-rotational and velocity strain formulation, and is computationally efficient. The penalty based contact algorithms were used to model the contact between the vessel and the braces, and the internal contact of the ship and the tube itself. A friction coefficient of 0.3 was assumed for all the contacts. In cases where both the ship and braces could deform, the ship model travelled with a prescribed constant speed of 1m/s and the braces/legs were clamped at both ends against 6DOF motions. For ship models colliding

with rigid tubes, the ship model was fixed against both translations and rotations, and the rigid tube moved in a prescribed path with a velocity of 1m/s. The ship bow and stern models are briefly introduced, and *more details are given in the appendix*.

3.2.1 Ship bow

The bulbous bow is from a typical modern supply vessel with a displacement of 7500 tons. Principal dimensions of the vessel are given in Table 2. The bow finite element model is shown in Fig. 5. The element size is generally 120 mm. The plate thickness varies from 7 mm for the decks to 12.5 mm in the bulb. The stiffener spacing is approximately 600 mm, with ring stiffeners and breast hooks of approximately 250 mm × 15 mm in the bulb. The bulbous part is almost cylindrical and is relatively strong. The forecastle protrudes 1.2 m ahead of the bulb.

Table 2. Principal dimensions of the supply vessel

Displacement	7500 tons
Length	91 m
Length between perpendiculars	79 m
Breadth	18.8 m
Depth	7.6 m
Draft	6.2 m

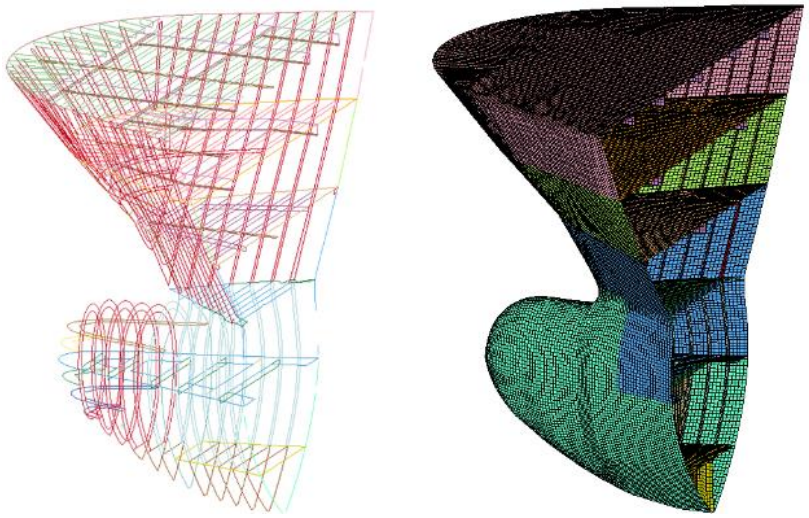

Fig. 5. The FE model of the bulbous bow

3.2.2 Stern No. 1

The stern No. 1 model was established from the same supply vessel described above. Half of the stern end was modelled for stern corner collisions, and the model was mirrored to obtain a full model for stern end collisions (see Fig. 6). The center girder was added after mirroring.

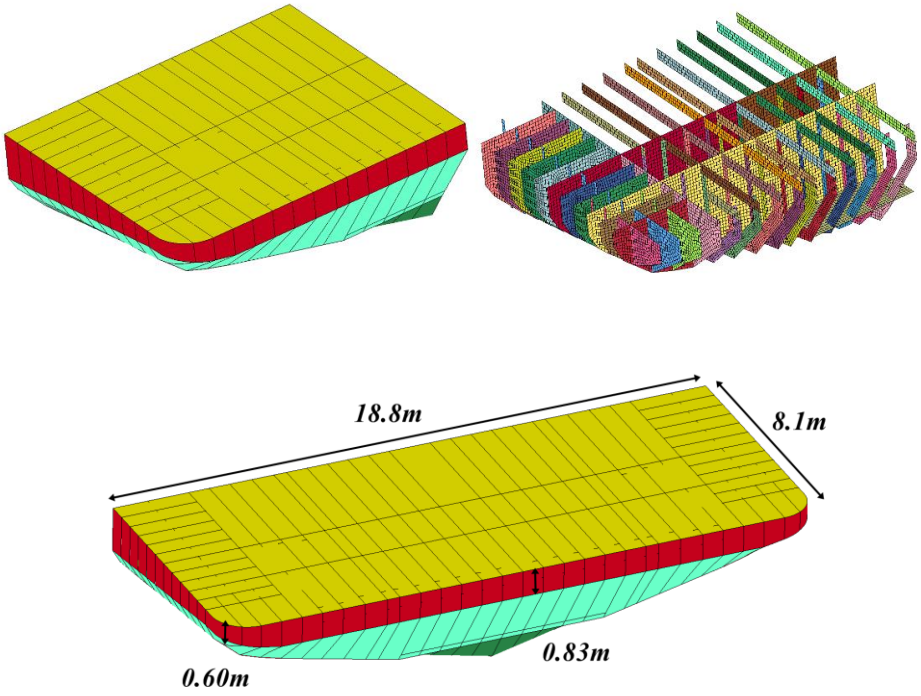

Fig. 6. The finite element model of stern No. 1

This stern model has a small vertical section, being 0.60 m at the stern corner and 0.83 m at stern end. The length of 8.1 m ensured sufficient energy absorption without violating the boundary conditions. The thickness is 11mm for the outermost plate and 15 mm for the deck plate. Transverse and longitudinal frames are located every 0.65 m with a plate thickness of 10 or 15 mm. The mesh size is typically 100 mm, giving an element size over shell thickness ratio ranging from 5 to 10.

3.2.3 Stern No. 2

The second supply vessel has a displacement of 7500 tons and a draught of 6.2 m. The stern end is 19 m wide and characterized by a large vertical section of 4.95 m (see Fig. 7). It is equipped with frames in both longitudinal and transverse directions with a spacing of 0.7 m. The web thickness is 9 mm. Manholes are included in the frame web. The outmost shell plates have a thickness of 12 mm, and are strengthened by stiffeners spaced every 0.7 m.

The half-stern model was mirrored for stern end-brace collisions and the main girder was added. The length of the model is 11.76 m. The mesh is relatively fine, with size typically in the range of 45-55 mm. This gives a mesh size/thickness ratio of 4-5.

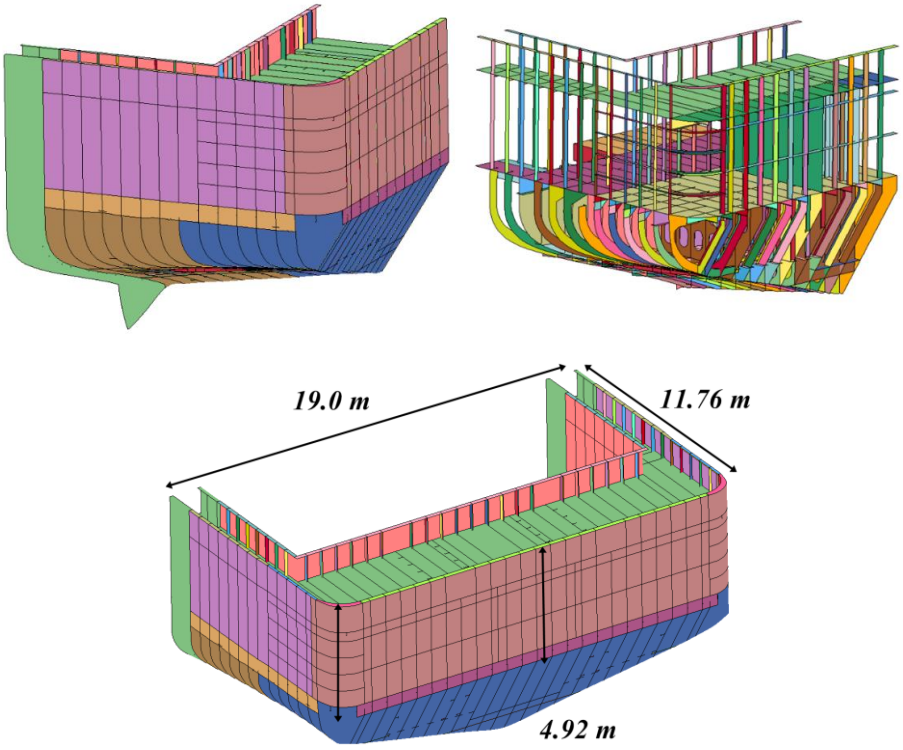

Fig. 7. The finite element model stern No. 2

4. Ship collision with rigid braces

4.1 Ship bow-rigid brace impact

The ship bow was first subjected to penetration by rigid braces oriented horizontally and diagonally. The brace diameter was 1 m. The contact locations are indicated in Fig. 8. The force curves are plotted in Fig. 9 along with a curve that was proposed by Amdahl [15] for a 5000 tons supply vessel colliding with a 1m-diameter brace on the stringer. This curve was derived by means of simplified plastic analysis.

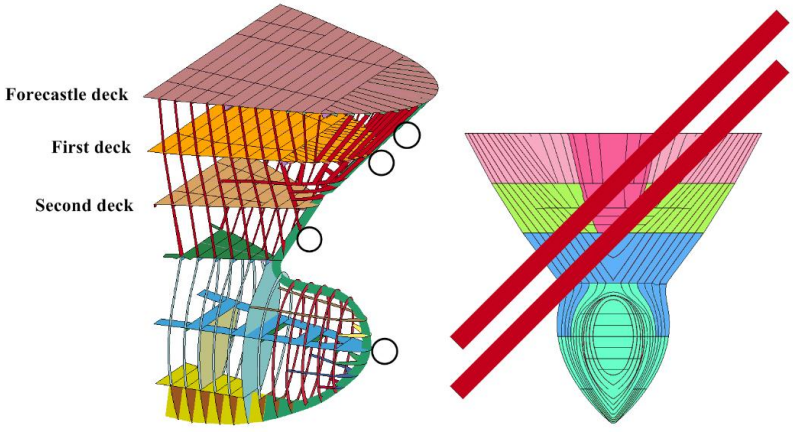

Fig. 8. Contact locations of the bow-brace collisions

The curve proposed by Amdahl [15] predicts the force levels reasonably well. The simulated forces for collision with the diagonal brace on the bow second deck are slightly larger. According to the present DNV-GL RP C204 standard [4], almost all the energy will go into the bow if the brace collapse load is larger than 10 MN. According to this simulation, it will have to be increased to 15 MN to account for larger vessel size. The resistance to penetration by vertical braces of this bow model was investigated by Storheim and Amdahl [22].

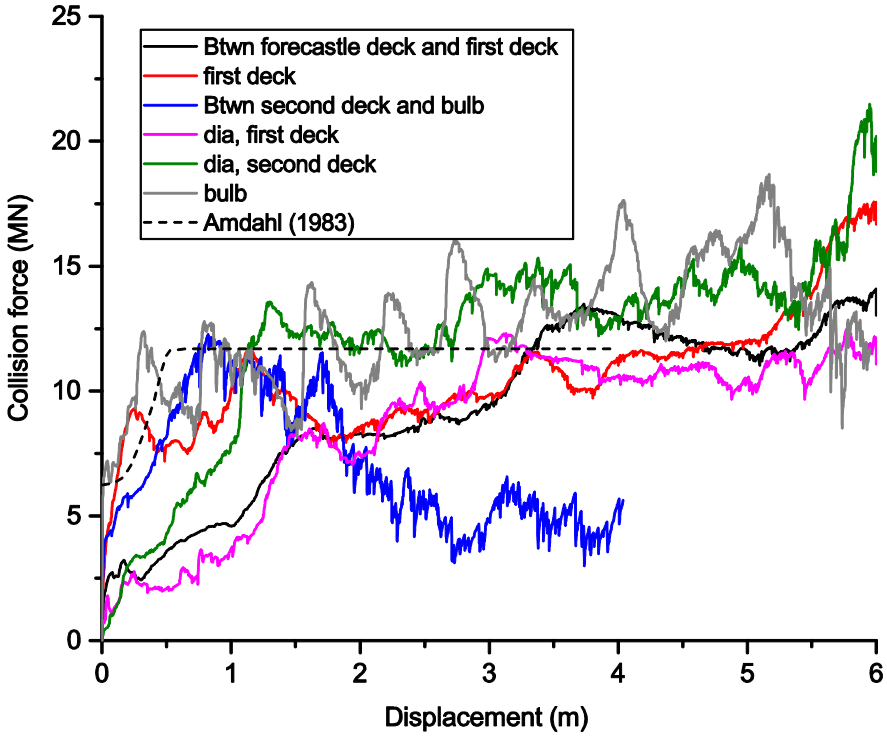

Fig. 9. Force-deformation curves for bow impact on 1 m diameter braces

4.2 Stern corner-rigid brace/leg impact

Penetration of stern corner by rigid braces/legs was investigated. The brace and leg diameter was 1.5 m and 10 m, respectively, in correspondence with the diameter behind the DNV-GL design curves. The resistance to penetration is plotted in Fig. 10 along with current design curves. The resistance for the stern 2 penetrated by a rigid 1.5m-diameter leg with a batter of 1:8 is also presented.

The contact height for stern 2 is much larger than that of stern 1, and a much larger collision force is therefore created. The force curve of stern 2 for 1.5 m-diameter rigid brace impact agrees well with the current DNV design curve. The initial forces may be somewhat exaggerated as full contact over the entire height is assumed. Unlike vertical brace collision, the resistance for the battered leg collision starts from zero and the maximum resistance is a little larger because of larger contact area.

The current DNV-GL RP C204 standard [4] does not cover collisions with a 10 m diameter rigid column. It is suggested that a design curve should follow the trend of the force displacement curve for stern 2.

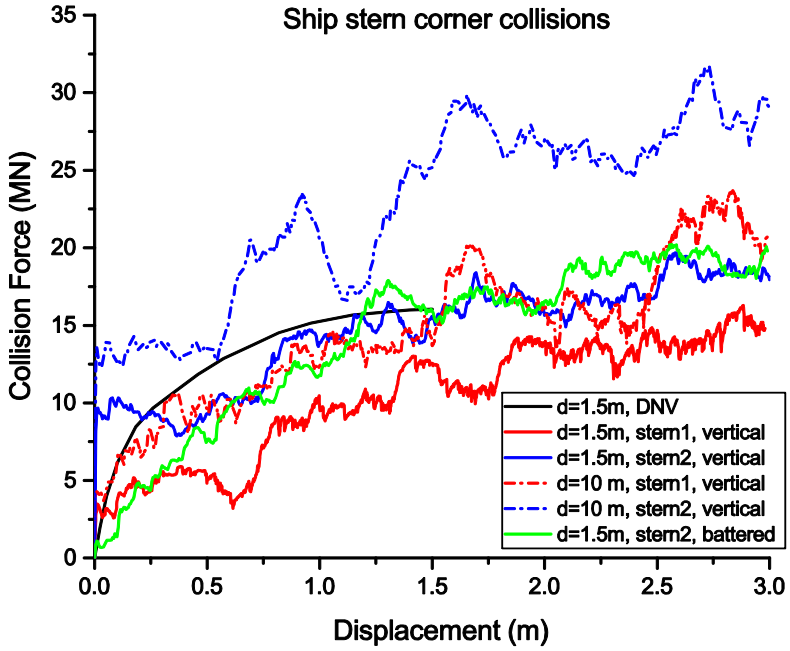

Fig. 10. Force-deformation curves for stern corner-rigid vertical brace collisions

4.3 Stern end-rigid brace impact

The stern end models were subjected to penetration by rigid vertical tubes with a diameter of 1.5 m and 10 m both in ship center line and at quarter width. Collision with a rigid jacket leg with a batter of 1:8 and a diameter of 1.5 m was also simulated. The force-displacement curves are plotted in Fig. 11 for stern 1 and in Fig. 12 for stern 2 respectively, along with current design curves.

The collision forces of stern 1 follow the design curves well up to 1 m deformation, but becomes substantially larger beyond 2 m penetration. The sudden drop at a displacement of about 1m is caused by shell plate fracture. The force level for stern 2 exceeds the design curves substantially. It is suggested that a design curve should follow the curves for the stringer vessel, i.e. stern 2.

For the 1.5 m rigid brace collisions, significant force drops are observed for center collision, but not for quarter width collisions. The drops for center collision are due to shell plating fracture and, more importantly, buckling of the main girder. Design curves for stern end impacts are suggested to follow the curves of stern 2 in Fig. 12.

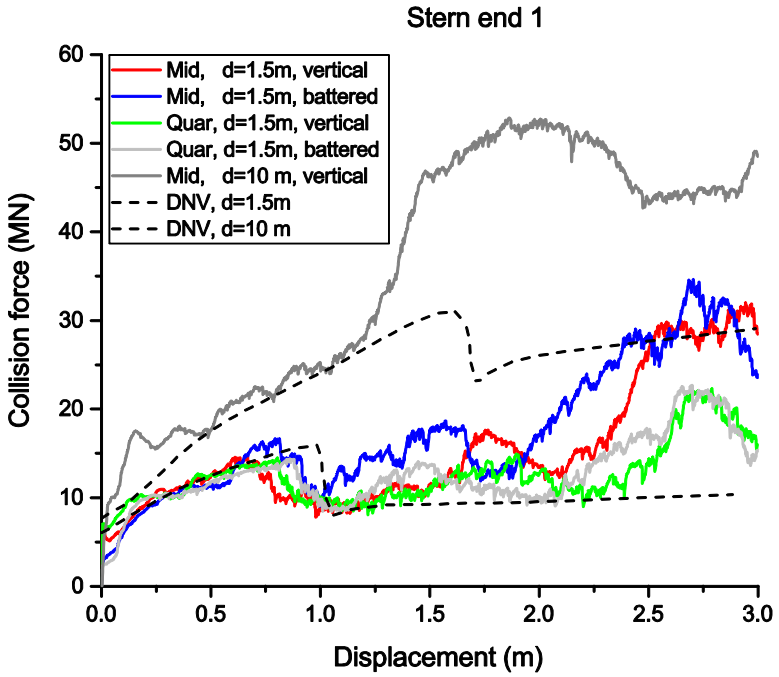

Fig. 11. Force-deformation curves for the end of stern 1 collision against rigid braces

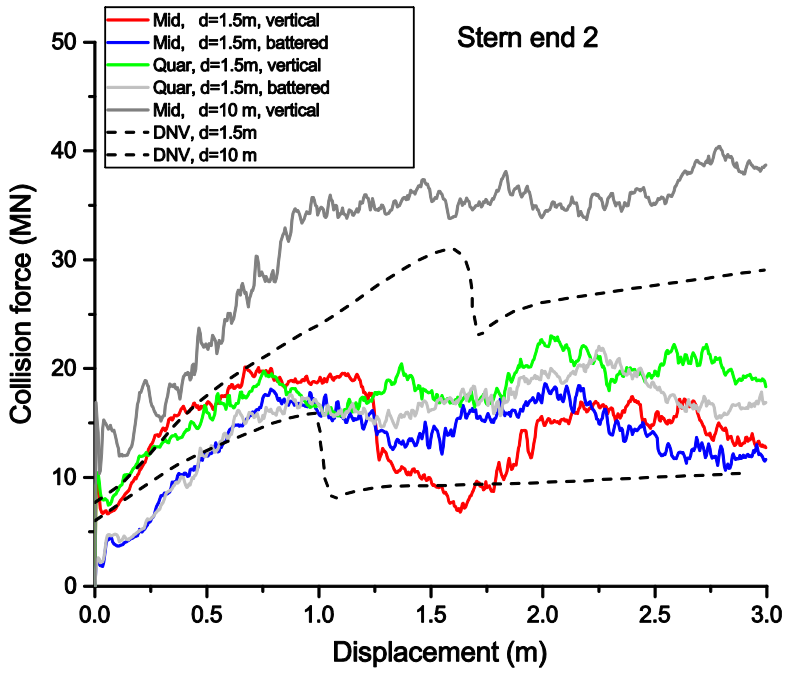

Fig. 12. Force-deformation curves for the end of stern 2 collision against rigid braces

5. Denting resistance of braces and legs subjected to lateral impacts

5.1 Denting resistance with rigid ship and deformable braces

Two flat rigid indenters were modeled with a contact width of 0.6 m and 4.92 m representing the initial contact width of stern 1 and stern 2, respectively (see Fig. 13). The tube had a length of 20 m, a diameter of 1.5 m and a thicknesses varying from 30 mm to 50 mm. The material with a yield stress of 285 MPa in Table 1 was used. The tube ends were fixed against motions.

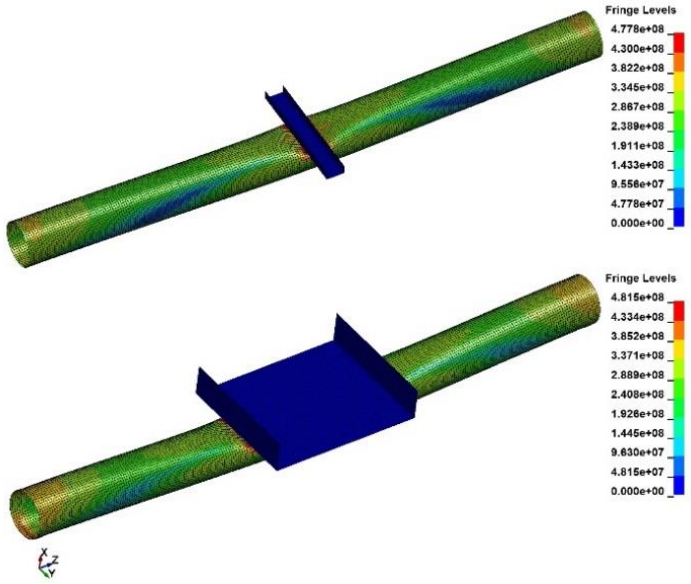

Fig. 13. Impact responses of tubes with rigid indenters of different sizes

The denting resistance predicted by the theoretical models reviewed in *Section 2.1* is compared with LS-DYNA simulations in Fig. 14 for a tube thickness of 40 mm. Local indentation is defined as the original tube diameter less the residual 'diameter' of the dented cross section. It shows that the denting models predict the resistance for small contact width reasonably well up to an indentation of 0.6 m. For larger indentation, the force grows drastically because the ends are assumed fully fixed against inward motion in the simulation, and the stiffening effect of membrane forces may be exaggerated.

A more detailed investigation of the NORSOK model, the Cho model and the modified Wierzbicki and Suh model considering the contact height effect is given in Figs. 15 and 16, where the tube wall thickness varies from 30 mm to 50 mm. The NORSOK and Cho models work generally well for small contact width, but underestimates the resistance when the contact width is large. The underestimation increases with increasing tube wall thickness. The modified Wierzbicki and Suh model is more accurate for both small and large contact widths. The contact width effect is well captured by the second term in Eq. (6), which enables the denting force to start from a nonzero value when the contact width is nonzero.

From Figs. 14-16, the denting resistance model is no more valid when the indentation is large, because the braces/legs start global bending and develop axial membrane forces. However, it is

easily observed that local denting continues to increase in the beam bending stage. This phenomenon will be discussed in more detail later.

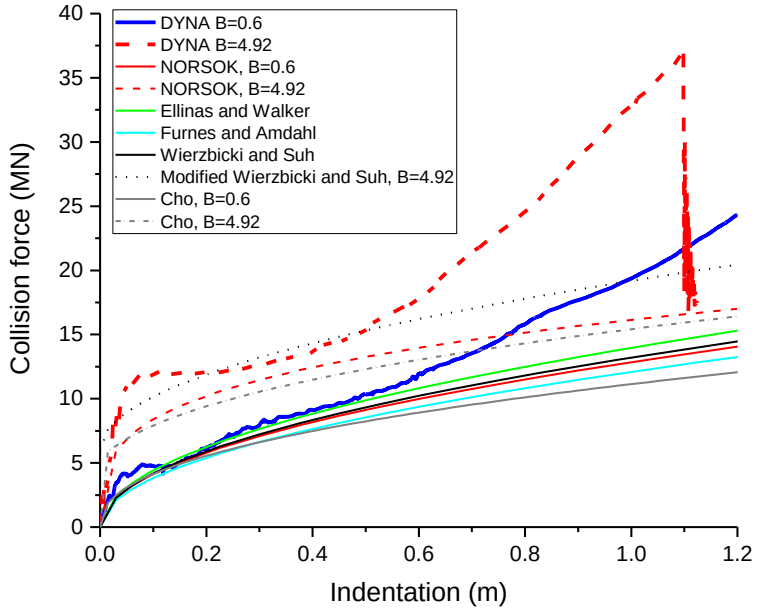

Fig. 14. Comparison of denting resistances by DYNA simulations and analytical models

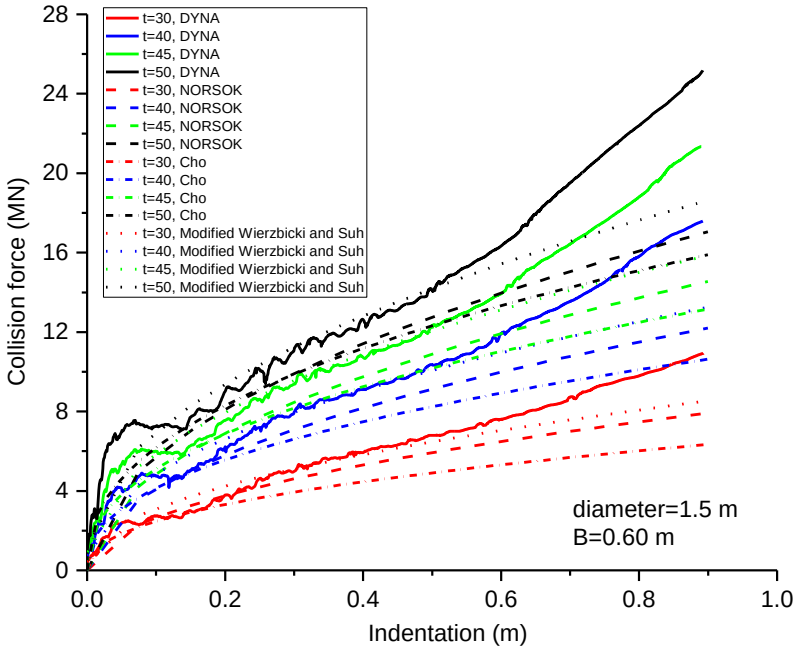

Fig. 15. Comparison of denting resistances from impacts of a rigid indenter with a contact width B= 0.6 m

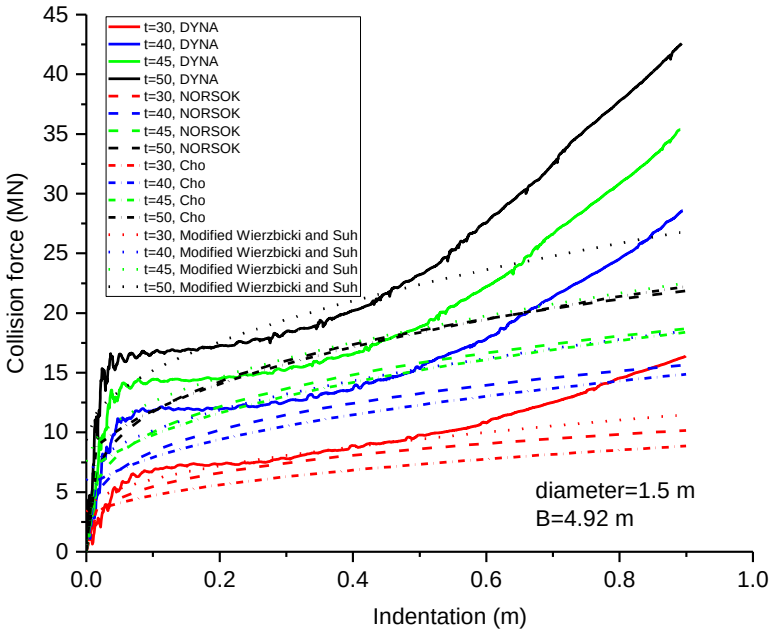

Fig. 16. Comparison of denting resistances from impacts of a rigid indenter with a contact width B=4.92 m

5.2 Denting resistance with deformable ship and braces

The NORSOK curve and the modified Wierzbicki and Suh model were investigated in the more realistic conditions where both the ship and braces are deformable. Stern corner impacts with a vertical brace were considered. The brace length was 20 m, the diameter was 1.5 m and the wall thicknesses varied from 30 mm to 50 mm. The material with a yield stress of 285 MPa was used. The resistance curves are plotted in Figs. 17 and 18. The dashed and dotted lines represent scenarios where the contact height is equal to the initial and maximum height of the stern corner for the two denting models, respectively.

The stern undergoes little damage when the thickness is 30 mm, but brace denting is substantial. Both models predict the denting resistance reasonably well. For braces with larger thicknesses, the denting resistance increases due to several effects. A strong brace (increasing thickness) may deform the ship and thus increase the contact height between the brace and the ship. In addition, the deforming stern will wrap around the brace as illustrated in Fig. 19, which increases the contact area. For the cases with increasing contact heights and wall thicknesses, the NORSOK model underestimates the denting resistance to some extent, while the accuracy of the modified Wierzbicki and Suh model is good.

If the brace deflection is in the order of brace radius, the denting resistance increases significantly due to membrane action and the design denting curves are no longer valid. The markers on the curves represent the time instant when the total energy dissipation is 30 MJ. The absolute values of the forces are quite similar, but the R/R_c value decreases with increasing wall thicknesses.

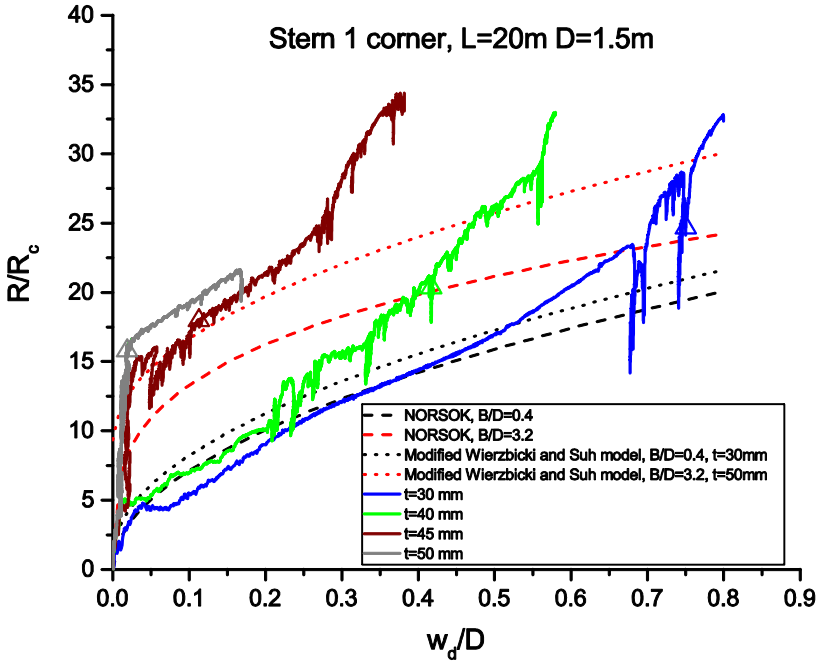

Fig. 17. Comparison of denting resistance from impacts of the stern 1 corner

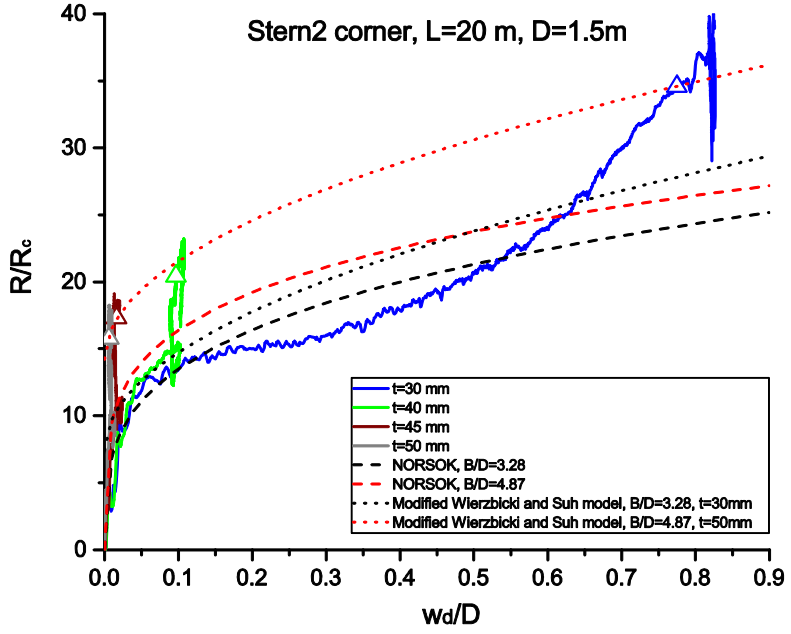

Fig. 18. Comparison of denting resistance from impacts of the stern 2 corner

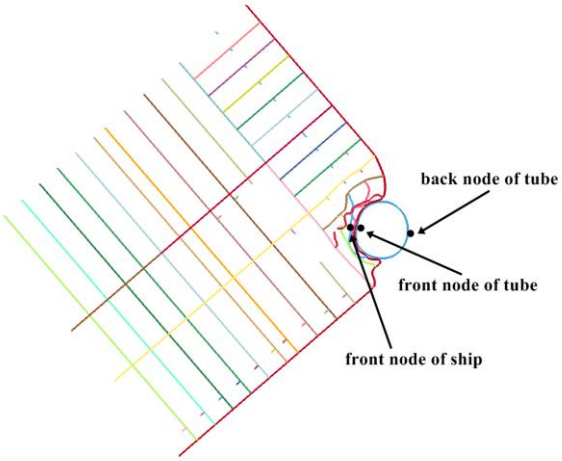

Fig. 19. Sectional view of the ship stern corner-brace collision

The simulations show that the denting resistance provided by both models is satisfactory, but the modified Wierzbicki and Suh model performs better for large contact height and thick-walled tubes.

6. Transition from local denting to global bending

6.1 The transition indentation ratio

A brace/leg deforms first by local denting. The local indention decreases continuously the plastic bending moment of the tube. At a certain indentation, $w_{d,tran}/D$, a transition takes place where the brace/leg starts to deform with a plastic mechanism. By further deformation, the resistance may remain constant, reduce or increase depending on the boundary conditions and the diameter over thickness ratio, see Fig. 20. If the braces are very thin-walled, local dent may grow significantly in the bending stage and the resistance is further reduced. If the boundaries are stiff against inward motion, the resistance may increase again after finite deformations due to the membrane action.

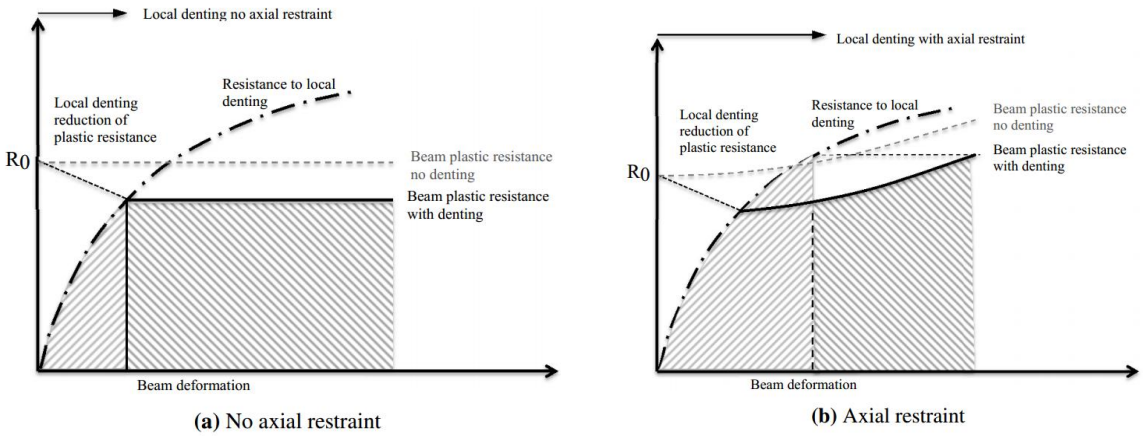

Fig. 20. Plastic resistance vs. beam deformation for varying axial restraint (From Storheim and Amdahl [22]).

A few researchers have studied the transition from denting to global bending in the derivation of the resistance to denting, bending and membrane stretching, but little discussion on the transition indentation ratio exists. De Oliveira et al. [25] proposed the following expression for the transition indentation ratio:

$$\frac{w_{d,tran}}{D} = 2(\lambda - \sqrt{\lambda^2 - 1}) \tag{12}$$

where

$$\lambda = 1 + \frac{\pi}{4} \cdot \left(\frac{L}{D}\right)^2 / \left(\frac{D}{t}\right) \tag{13}$$

According to Ellinas and Walker [12], the transition indentation ratio can be found by solving the following equations:

$$\frac{w_{d,tran}}{D} = \left[16/K \cdot \frac{D}{L} \cdot \frac{D}{t}(1 + \cos\beta - \beta)\right]^2 \tag{14}$$

where

$$\beta = \left[1 - \frac{D}{t}\left\{\sqrt{16/9 \cdot \left(\frac{w_{d,tran}}{D}\right)^2 + \left(\frac{t}{D}\right)^2} - 4/3 \cdot \frac{w_{d,tran}}{D}\right\}\right] \cdot \sqrt{\frac{w_{d,tran}}{D}} \tag{15}$$

and K is as defined in Eq. (7). Neither model accounts for the contact width. If we combine the relatively conservative NORSOK denting model (eq. (2)) and the NORSOK residual plastic bending-capacity model (Eqs. (9) and (10)), we will obtain a new expression for the characteristic transition indentation ratio $w_{d,tran}/D$ by solving:

$$\frac{R_0}{2R_c}\left(1 + \sqrt{1 - \frac{w_{d,tran}}{D}} - \sqrt{\frac{w_{d,tran}}{D} - \left(\frac{w_{d,tran}}{D}\right)^2}\right) = \left(22 + 1.2\frac{B}{D}\right)\left(\frac{w_{d,tran}}{D}\right)^{\frac{1.925}{3.5 + \frac{B}{D}}} \tag{16}$$

For a brace with clamped ends, R_0/R_c can be expressed as:

$$R_0/R_c = 32\sqrt{\frac{D}{t}} \cdot \frac{D}{L - B} \tag{17}$$

$L - B$ is the effective brace length that is used to determine R_0. It is found that $w_{d,tran}/D$ depends only on two parameters, i.e. R_0/R_c and B/D. This dependence is consistent with De Oliveira et al. [25]'s model in Eqs. 12 and 13 when B=0.

The transition indentation ratios predicted by the three models are compared with numerical simulations in Table 3. The ship does not deform much prior to beam bending for the cases in Table 3. Otherwise, the instantaneous contact width will be difficult to measure in the numerical simulations. The output intervals of nodal displacements was set to 0.01m to capture accurately the transition from local denting to beam bending. The transition indentation in the numerical simulations is defined as the indentation where the nodes on the rear side of the tube move with a velocity of no less than 10% of the ship rigid motion velocity and deform continuously afterwards with the same or larger speed. This definition is believed reasonable because the rear side of the struck tube will contract a little in the denting phase due to ovalization of tube cross sections (see Fig. 21), and the nodal velocity on the rear side will thus not be continuously increasing. The existence of cross sectional ovalization and rear side contraction during local denting have been identified in experiments by Amdahl [9] and Jones et al [16], and were considered in the analytical model by Jones and Shen [13].

It is found that all three models provide reasonably accurate predictions of $w_{d,tran}$ /D for varying tube length, diameter and thickness. De Oliveira et al. [25] model agrees best with numerical results. The proposed model has the advantage of accounting for the contact length.

A significant discrepancy is observed for stern 1 corner collisions against leg geometry 20 ×1.0 ×20 (length[m] × diameter[m] × thickness[mm]). This may be because the denting resistance should start with a certain nonzero force level as indicated by the modified Wierzbicki and Suh model in Eq. (5). Numerical simulation results show that there is a threshold $w_{d,tran}$/D value of 0.15, below which a brace/leg experiences negligible local denting before initiation of global bending.

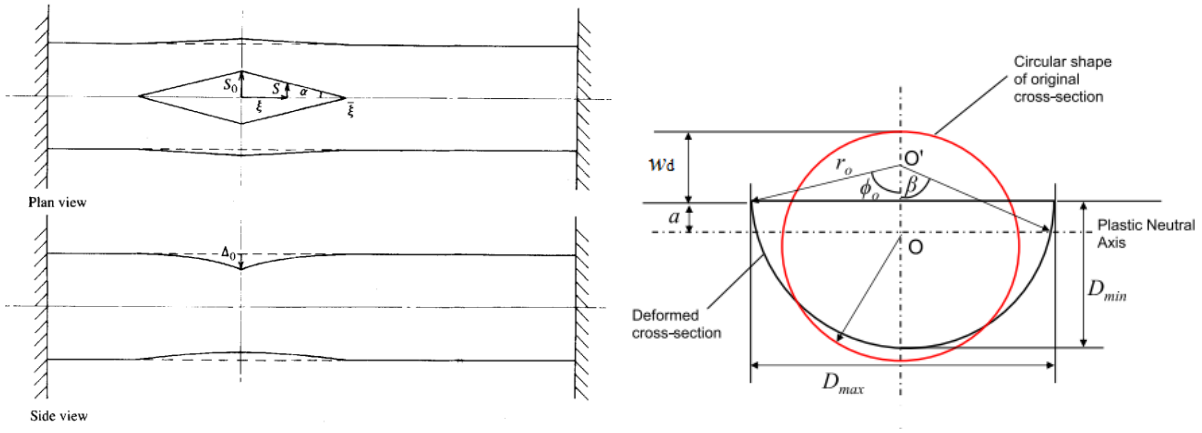

Fig. 21. Deformation of brace cross sections during indentation (from Jones and Shen [13], Jones et al [16] and Cerik et al. [23])

Table 3. Verification of the analytical models for transition indentation ratios

Striking ship	Brace dimension L(m)xD(m)xt(mm)	Simulated $w_{d,\,tran}/D$	Proposed method	Ellinas and Walker [12]	de Oliveira, Wierzbicki [25]
Stern 1 corner	20x1.0x20	0.008	0.138	0.167	0.138
Stern 1 corner	20x1.2x20	0.183	0.222	0.273	0.218
Stern 1 corner	20x1.0x30	0.133	0.160	0.158	0.156
Stern 1 corner	20x1.5x30	0.233	0.276	0.289	0.268
Stern 1 corner	20x1.6x20	0.388	0.424	0.512	0.411
Stern 1 corner	20x1.8x30	0.350	0.410	0.436	0.397
Stern 1 corner	10x1.5x20	0.833	0.942	0.795	0.788

Fig. 22 shows the variation of the transition indentation ratio for a large range of L/D and D/t values using De Oliveira et al. [25] model. It is found that the large transition indentation ratios are concentrated in the region with small L/D and large D/t values. The ratio shows the dominant deformation pattern (local denting or global bending) for braces and legs with certain dimensions and material properties, and helps to understand how they behave during collisions.

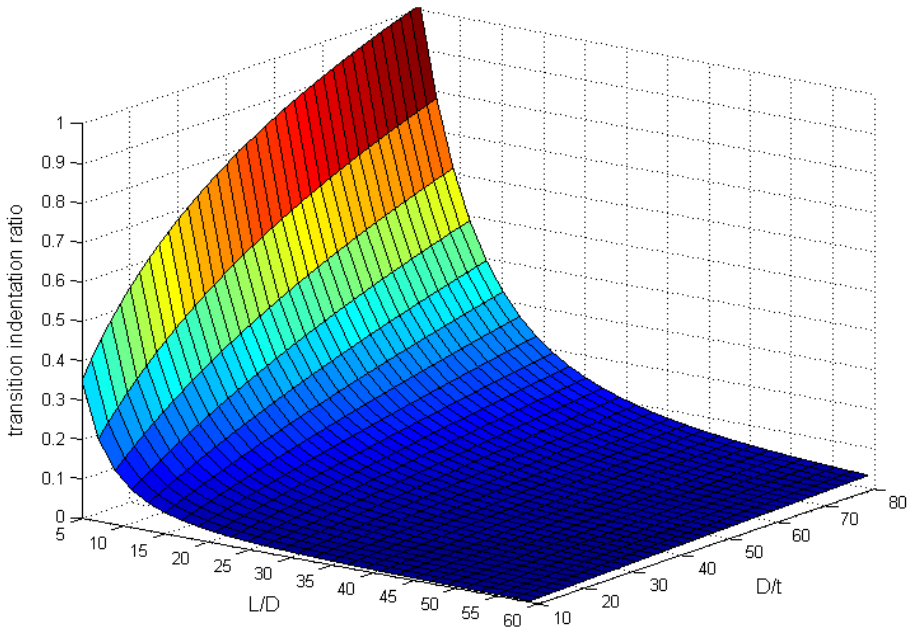

Fig. 22. Variations of transition indentation ratios with L/D and D/t

The transition indentation ratio is calculated for a few representative ship-brace collisions based on the proposed model, refer Table 4. The ratio will decrease with increasing wall thickness, i.e.

the brace will be subjected to less denting with large brace thickness. In addition, $w_{d,tran}/D$ values are found to decrease significantly for decreasing brace diameters and increasing brace lengths. The variations of $w_{d,tran}/D$ with wall thickness, diameter and length are reflected in eq. (17), where R_0 / R_c varies with the powers of $\frac{3}{2}, -\frac{1}{2}$ and -1 for the diameter, thickness and length of a brace/leg, respectively. Another important factor is the contact width B. On one hand, the contact width reduces the effective length in calculating R_0 and therefore gives a larger R_0 / R_c and subsequently a larger $w_{d,tran}/D$; on the other hand, the capability to resist local denting is enhanced with increasing contact width and this will reduce the $w_{d,tran}/D$. The tendency of decreasing $w_{d,tran}/D$ with increasing contact widths seems to be dominant

Table 4. The $w_{d,tran}/D$ values for different cases

Striking ship	Brace dimension L(m)x D(m)xt(mm)	$w_{d,tran}/D$	R_0(MN)	R_c (MN)	R_0/R_c
Stern corner 1	20x1.2x30	0.16	4.78	0.41	11.78
Stern corner 1	20x1.2x40	0.12	6.26	0.62	10.02
Stern corner 1	20x1.2x50	0.10	7.69	0.87	8.81
Stern corner 1	20x1.5x30	0.28	7.54	0.45	16.63
Stern corner 1	20x1.5x40	0.22	9.92	0.70	14.21
Stern corner 1	20x1.5x50	0.18	12.22	0.97	12.53
Stern corner 1	10x1.5x30	0.71	15.40	0.45	33.95
Stern corner 1	20x1.5x40	0.59	20.25	0.70	29.01
Stern corner 1	20x1.5x50	0.50	24.97	0.97	25.59
Stern corner 2	20x1.5x30	0.20	9.80	0.45	21.61
Stern corner 2	20x1.5x40	0.14	12.89	0.70	18.47
Stern corner 2	20x1.5x50	0.10	15.89	0.97	16.29

6.2 Discussion of compactness criteria

The existing compactness criteria and the transition indentation are connected. The R_0 / R_c value in Eq. 17, depends on D/ (L-B) and D/t. If we assume conservatively that the contact width $B = 0$, it is interesting to find that the R_0 / R_c compactness criterion according to the NORSOK standard [3] and Cerik et al. [23], and the D/t, L/D criterion by Sherman [17] are similar, and by the very nature limits $w_{d,tran} / D$ to be within a certain range as indicated in Table 5. The API rules set limits only to the D/t values, and may not be sufficient to ensure compactness.

Table 5. The compactness criteria

	Sherman	Cerik et al.	NORSOK
Compactness criteria	D/t⩽35; L/D⩾22	R_0/R_c⩽6.5	R_0/R_c⩽6
Corresponding R_0/R_c	R_0/R_c⩽8.6	-	-
Corresponding w_{tran}/D	w_{tran}/D⩽0.12	w_{tran}/D⩽0.08	w_{tran}/D⩽0.07

The question arises: Is it sufficient to limit the transition indentation ratio $w_{d,tran}/D$ to keep the cross sections compact during the beam bending phase? No, it is not; for stern corner 1 collision with the 20 ×1.0 ×20 (length[m] × diameter[m] × thickness[mm]) tube, where the simulated $w_{d,tran}/D$ is only 0.008, local denting increases continuously during global bending as demonstrated by the plots in Fig. 23. Continuous increase of local denting is also observed for stern corner 1 collision with 20 ×1.6 ×20 tube where the transition indentation is large ($w_{d,tran}/D$ = 0.39), see Fig. 24. The large membrane forces created by axially fixed ends may exaggerate local indentation, but the simulations do prove the insufficiency of using the transition indentation ratio as the compactness criterion. In addition, the rear side deflection of the brace in Fig. 24 is slightly negative in the denting phase, and this confirms the ovalization and contraction effect.

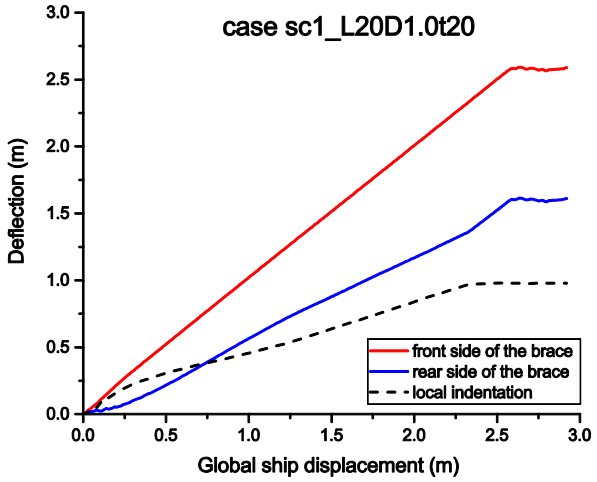

Fig. 23. Deflection curves of nodes on the front and back sides of the brace for case sc1l20d1.0t20

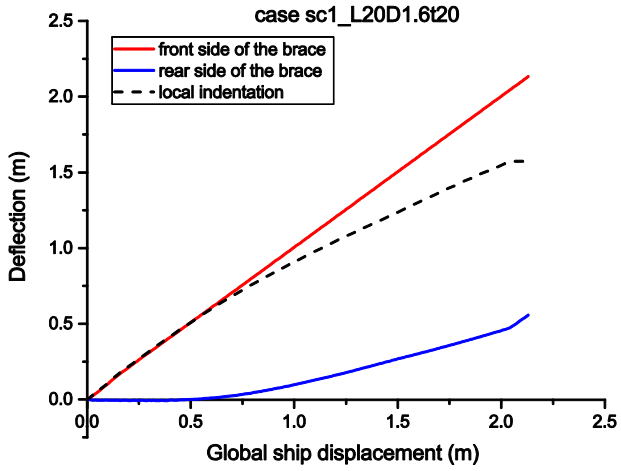

Fig. 24. Deflection curves of nodes on the front and back sides of the brace for case sc1l20d1.6t20

To guarantee compactness, the tube should be able to resist locally a certain force level for an indentation of, say for example 0.1D. This means that R_c should be larger than a certain value according to Eqs. (2) and (6) as proposed by Storheim and Amdahl [22]. They showed that the $R_0 / R_c < 6$ compactness requirement in NORSOK for bow-brace collisions was too conservative. However, we find that the criterion itself is not necessarily conservative. Another requirement that is often assumed for strength design is that the plastic bending capacity of the brace R_0 should be no less than the maximum collision force $F_{\max}$ when the ship crushes into a rigid brace/leg, i.e. $R_0 \geq F_{\max}$. By satisfying both requirements, we obtain:

$$R_c \geq \frac{F_{\max}}{6} \tag{18}$$

It is actually the combined requirement in Eq. (18) that is overly conservative.

Although the transition indentation ratio is not suitable as a compactness requirement, it is still useful for better understanding and prediction of the impact responses of braces/legs. For each brace/leg with specified parameters, a transition $w_{d,tran}/D$ from denting to bending can be determined. A brace will not start beam bending until the transition indentation is reached. This means for cases where the transition w_d/D is for example 0.2, only half of the full plastic bending capacity is maintained according to Fig. 4 (the model for residual bending capacity is conservative) when the brace starts to bend. The residual bending capacity may not be enough to resist the accidental collision loads and energy dissipated by further bending in the dented zone is limited. A large deflection of the brace may occur and affect the adjacent members. The load bearing capacity of the tube is further reduced if a leg carries axial compressive loads. However, the axial force level is normally moderate and the platform may often redistribute the axial force from a damaged leg to other legs through diagonal braces.

For cases with even larger $w_{d,tran}/D$, say 0.5, the brace can hardly dissipate any energy by bending in the dented zone, but only at member ends. The energy dissipated only by local denting is substantial but will not be enough to compensate for the loss in bending energy. It is not recommended to design legs such that they undergo extreme denting (say > 0.5D) as the resistance models become uncertain.

7. Design of offshore tubular members against ship impacts

The design of platform braces/legs against ship impact may be carried out in the ductile, shared-energy or strength design domain. The governing factor is the resistance to plastic collapse in bending, R_0. If the resistance is larger than the force that the ship will produce when penetrated by a rigid tube, the ship will predominantly dissipate the collision energy, i.e. the brace/leg response is in the strength domain. Normally, the collapse in bending is calculated for a “perfect” circular pipe, which is representative for pipe with no or small dents. In order for this to be valid, the brace/leg must comply with compactness requirements, R_c, with respect to local denting. In addition to reducing R_0, any denting will also increase the ship force, because the resistance to penetration of the ship is larger for a dented pipe than a rigid pipe.

If R_0 is less than the ship's resistance to penetration, the brace/leg will be in the shared-energy or ductile domain with small or no contribution to the energy dissipation from the ship. Depending on the dimensions and material strength, the brace/leg may dissipate considerable energy by beam bending and later by membrane forces at large deformations provided that the ends have some restraint against inward motion. Any local denting will contribute to the energy dissipation as well and may be included as described in Figure 20. However, it may be advisable to avoid significant local denting for two reasons:

1. With little local denting, simple plastic beam theory applies
2. Local denting reduces the energy dissipation, and the resistance of sections dented beyond brace/leg radius is uncertain

On the other hand, denting plays a less role in membrane stage, because the axial capacity is in principle not impaired.

A new compactness criterion, R_c, that depends on the maximum collision resistance of the ship bow penetrated by rigid braces/legs, F_{max}, is suggested for bow-brace collisions:

$$R_c \geq 1.9 \frac{F_{\max}}{24} \tag{19}$$

F_{max} can be read directly from the design curves. The validity and accuracy of the criterion is investigated by simulation of bow collisions. The required R_c values for stern corner and end collisions are also studied.

7.1 Bow collisions

Force-penetration curves for rigid braces with 1.0 m diameter and a yield strength of 420 MPa were presented in Figure 9. The maximum force for horizontal impact on first deck was 12 MN but the force attained 9 MN after only 0.2 m penetration. The force for diagonal brace impact on the first deck increased steadily to 12 MN after 3 m penetration. For diagonal brace impact on second deck, the force level was 13 MN after 1.4 m, and increased to 15 MN after 3 m.

The question is: How shall we determine the collapse resistance R_0? Penetration forces generated in early stages of penetration may be reasonably modeled as concentrated forces, but for large penetrations, it is justified to account for the increase of contact width. A possible model could be to reduce the effective brace length.

A few cases have been simulated, where the pipe thickness of 44 mm has been determined from the compactness requirement in Eq. (19) based on a maximum contact force of 12 MN. The collapse load R_0, based on a concentrated load and no denting, was varied by adjusting the brace length. In addition, the collapse load was calculated using the effective brace length after 3 m deformation, see Table 6.

Based on these values, we expect impacts on horizontal braces with a length of 11.2 m and 13.5 m will fall in the strength domain as the calculated R_0 values are both larger than the demand. For 16.8 m long braces/legs, beam collapse may occur as the resistance is slightly lower than the demand. With a length of 22.5 m, the response should be pushed very much to the ductile domain.

Similarly, diagonal impact on first deck should be in the strength domain, but it is more difficult to judge second deck impact; it could be in the shared energy domain because the resistance may not be sufficient to meet the demand for 13 MN after and the compactness requirement is not entirely fulfilled.

Table 6. Bow collision with braces

Brace position	F_{max} (MN)	Brace/leg dimension L(m)x D (m)xt (mm)	R_c (MN)	R_0 (MN) concentrated	Effective R_0 after a crushing distance of 3 m (MN)
Horizontal, first deck	12	11.2x1.0x44	0.95	12	21.8
Horizontal, first deck	12	13.5x1.0x44	0.95	10	15.9
Horizontal, first deck	12	16.8x1.0x44	0.95	8	11.5
Horizontal, first deck	12	22.5x1.0x44	0.95	6	7.7
Diagonal, first deck	12	16.8x1.0x44	0.95	8	13.1
Diagonal, second deck	15	16.8x1.0x44	0.95	8	17.2

The deformation mode after a total energy dissipation of 30 MJ for horizontal brace impact on first deck is illustrated in Fig. 25 for R_0=12 MN and R_c=0.95 MN. The brace penetrates ship bow with minor denting and beam deformation; the response belongs to the strength domain.

The resistance versus local denting and beam deformation of brace as well as bow penetration as a function of R_0 is plotted in Fig. 26. Minor denting and beam deformation of brace takes place when R_0= 12 MN and 10 MN. This witnesses strength design behavior where the brace penetrates deeply into the bow. For R_0 = 8 MN, and 6 MN, the brace is still capable of penetrating the bow significantly, but the brace suffers increasing local denting and beam deformation. The behavior can be categorized as shared energy response.

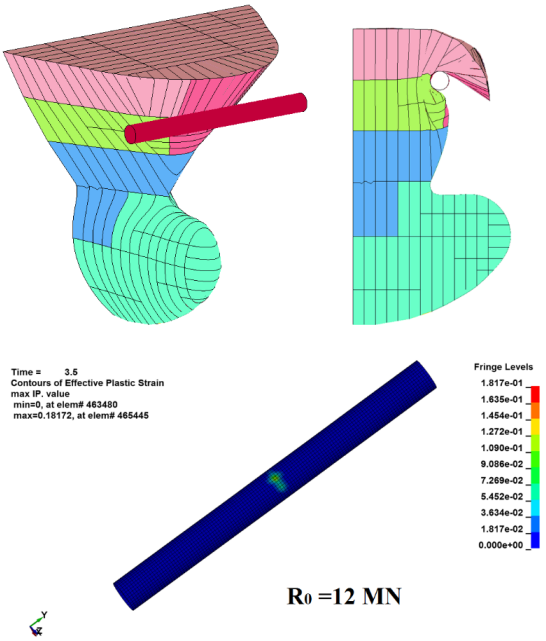

Fig. 25. Deformation mode for first deck impact against a horizontal brace, R_0=12 MN

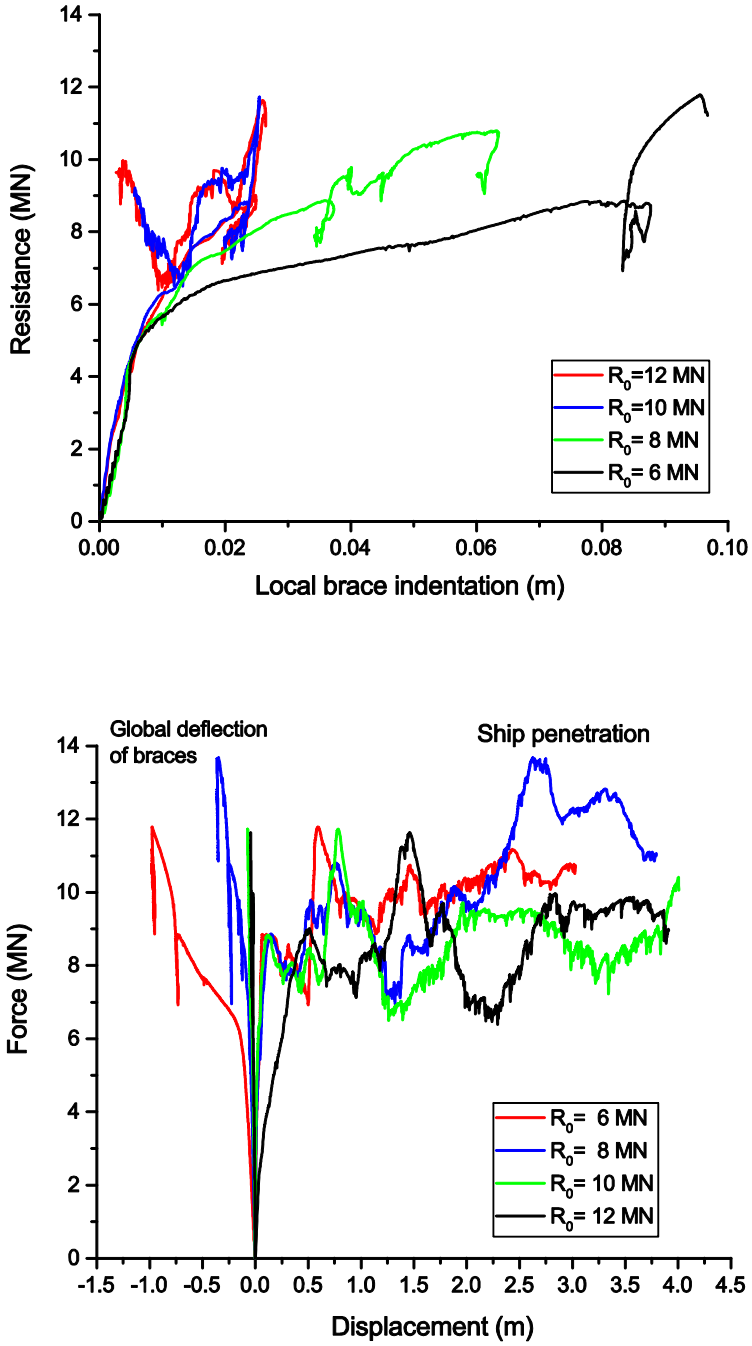

Fig. 26. Resistance versus: Local denting (top) and beam deformation and ship indentation (bottom) as a function of plastic collapse load R_0

For diagonal brace collisions, the deformation of the ship bow and braces is illustrated in Fig. 27 for a total energy dissipation of 30 MJ. The ship bow is found to deform significantly and absorb considerable energy. The distribution of equivalent plastic strains on the braces is shown in Fig. 28. The brace in first deck collision case undergoes a local indentation of 0.14 m and dissipates

3.0 MJ. Virtually no strain is observed at the brace ends, meaning that collapse by plastic bending does not occur. Hence, we consider it justified categorizing it as strength domain response. For second deck collision, the brace denting is 0.22 m and dissipates about 6.3 MJ. Moderate plastic strains are observed at the ends as the brace has started to form a three-hinge mechanism; the response falls now into the shared-energy domain..

It is challenging to provide quantitative information on brace effective length during continuous penetration. In lieu of more detailed calculations, it is recommended to assume conservatively a point loading in calculating R_0; the increasing contact width during penetration of the bow provides a safety margin to the brace strength.

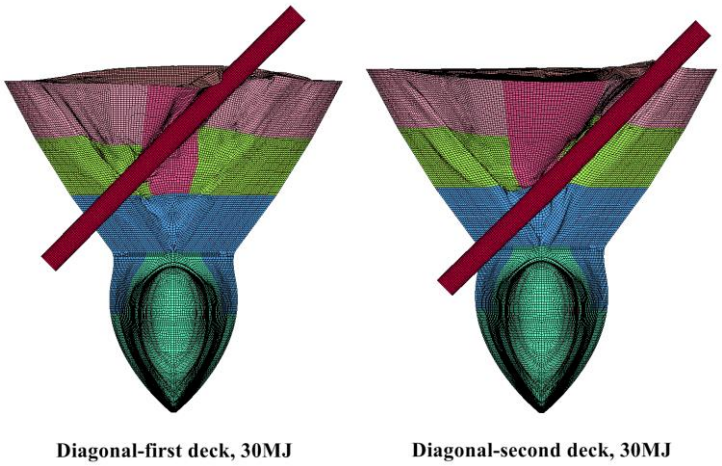

Fig. 27. Deformation mode for first and second deck impact against a diagonal brace, R_0=8MN

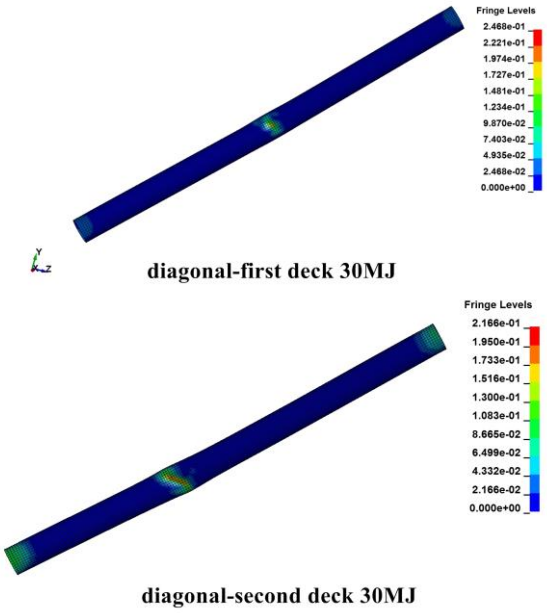

Fig. 28. Equivalent plastic strains of the deformed braces with energy dissipation of 30 MJ

7.2 Stern corner collisions

Force deformation curves from simulation of stern corner 1 and stern corner 2 impacts on a vertical brace with 1.5 m diameter and varying thicknesses are plotted in Figs. 29 and 30. The brace length is 20 m. The collision force is plotted versus local denting and beam deformation of the brace as well as penetration of the stern end. The plastic collapse resistance for an undented brace, R_0, is indicated in the diagrams. The effective beam length is reduced for stern end 2 to account for the large contact height (4.92 m). For stern corner 1, a concentrated contact force is assumed.

Figs. 29 and 30 show that the effect of ship-platform interaction is significant. During collisions, the softer structure will deform and the impact force will be distributed over a larger contact area. This increases the resistance of the strong structure, and therefore there will be an upward shift of the resistance curve for the stronger structure. In collision checks of offshore platforms, load-deformation curves of ships and platforms are often established independently by disregarding the relative strength and assuming the other object as infinitely rigid. Shared energy design based on such force curves may not give the correct energy distributions.

When the thickness is 30 mm, the brace undergoes severe denting and large beam deformation for stern corner 1 impacts as shown in Fig. 29. The plastic bending mechanism develops when the force exceeds 5 MN, but membrane action compensates for the loss of plastic bending capacity. The denting increases the resistance of the stern corner, which is not penetrated before the force level exceeds 10 MN. At this point, the brace has deflected 0.75 m in bending in addition to 0.9 m local denting. If this can be achieved without fracture, significant energy is also dissipated in the stern. The maximum force during the simulation is 13 MN. At this stage, the brace has a dent of 1.2 m.

For a brace thickness of 40 mm, local denting is still significant, but the stern corner resistance to penetration decreases to 7.5 MN. Beyond this force level, the brace penetrates the stern corner, but as expected, it develops also a plastic mechanism for a force level of approximately 10.6 MN. The behavior can be characterized as shared energy response.

With a thickness of 45 mm, the brace undergoes little denting and the stern corner resistance is virtually identical to rigid brace impacts; the stern is penetrated continuously when the force increases beyond 5 MN. The brace dissipates little energy before the force reaches the plastic mechanism load of 13.2 MN. If the demand for energy dissipation is complied with at this force level, the requirements for strength design have been met. Within the range of deformations that have been simulated, larger brace thicknesses yield strength design.

For stern corner 2 impacts, 30 mm brace thickness yields significant local denting and global bending of brace. Because the tube is dented, the force must exceed 16.6 MN before the brace starts penetrating the stern corner. With global deformation of 1 m, the brace resistance is dominated by membrane action. For brace thickness equal to 40 mmm, the initial stern resistance decreases to 11 MN and for 45 mm, it is virtually identical to rigid brace impact. If the demand for energy dissipation does not call for force levels exceeding the mechanism load of 17 MN

strength design is achieved with 45 mm thickness. Thus, for both stern corners, the resistance to local denting may be satisfied for 45 mm brace thickness.

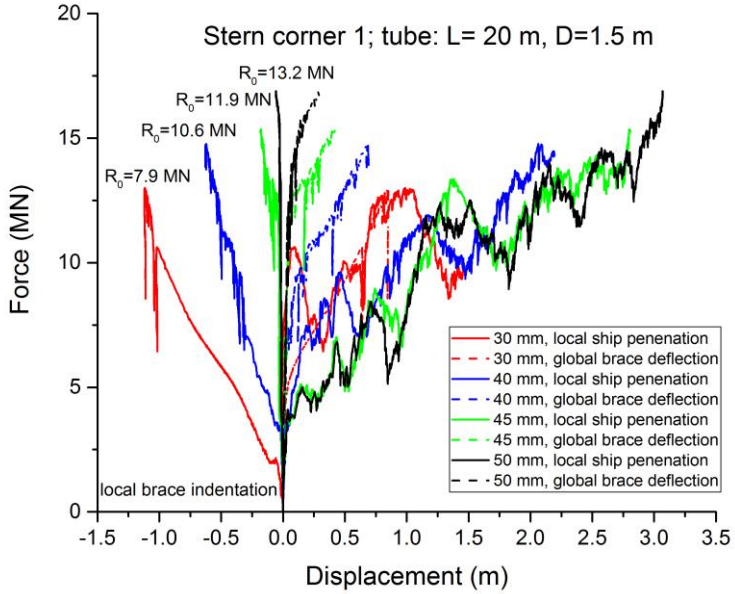

Fig. 29. Force versus local indentation and beam deformation of brace and force-versus penetration of stern corner 1 -vertical brace with 1.5m diameter and varying thicknesses

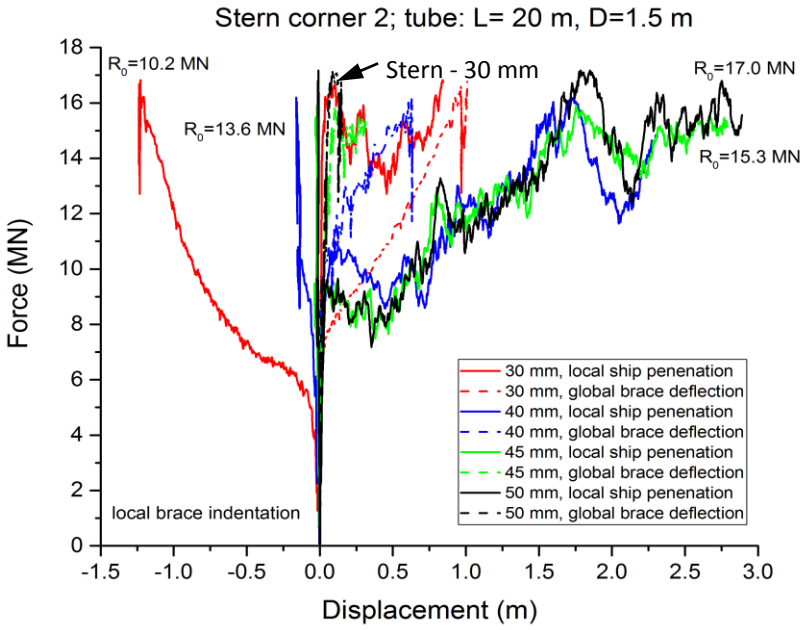

Fig. 30 Force versus local indentation and beam deformation of brace and force-versus penetration of stern corner 2 - vertical brace with 1.5m diameter and varying thicknesses

The required R_c values to maintain compactness of brace and leg cross sections are summarized in Table 7. For pipes with small diameters, such as the 20 ×1.2 ×50 (length[m] × diameter[m] × thickness[mm]) brace in Table 7, local denting can be disregarded during deformation, but R_0 is smaller than the ship penetration resistance. The brace will bend maintaining almost full bending capacity, and it will be pushed into the membrane domain in order to crush the ship. For cases with large diameters, by also satisfying the R_c criterion, R_0 is larger than the ship penetration resistance. The brace will be subjected to little local denting and global deflection, and most energy is absorbed by the ship deformation, known as strength design.

According to Table 7, the required thickness shows little diameter dependency for the two sterns. This observation agrees with the modified Wierzbicki and Suh model in eq. (5). When B is zero, the resistance given by eq. (5) is independent of tube diameter. For cases with large contact widths, the ship penetration resistance increases, and this may be compensated for by increasing the resistance to local denting. Based on the simulation results, R_c = 1.2 MN is recommended for stern corner impacts to be conservative.

Table 7. The required R_c values for different stern corner collision scenarios

Striking ship	*Brace dimension L(m)× D(m)*	*The required tube thickness t (mm)*	*Corresponding R_c (MN)*	*Corresponding R_0 (MN)*
Stern corner 1	20×1.2	50	0.87	7.8
Stern corner 1	20×1.5	50	0.98	12.4
Stern corner 1	20×1.8	45	0.91	16.3
Stern corner 1	20×2.0	50	1.12	22.3
Stern corner 1	10×1.5	45	0.83	23.1
Stern corner 2	20×1.5	45	0.83	12.9
Stern corner 2	20×2.0	45	0.96	26.0

7.3 Stern end collisions

Force deformation curves from simulation of stern end 1 and stern end 2 impacts on a vertical brace with 1.5 m and 2.0 m diameter and varying thickness are plotted in Figs. 31, 32, and 33. The brace length is 20 m. The collision force is plotted versus local denting and beam deformation of the brace as well as penetration of the stern end. The plastic collapse resistance for an undented brace, R_0, is indicated in the diagrams. The effective beam length is reduced for stern end 2 to account for the large contact height (4.92 m). For stern end 1 a concentrated contact force is assumed.

When the thickness is 30 mm, the brace undergoes severe denting and large beam deformation for stern end 1 impacts as shown in Fig. 31. At maximum force, the cross-section is virtually flat and the brace acts predominantly by membrane tension, because the ultimate collapse resistance in bending (R_0 =7.9 MN) is small. The stern is not penetrated, even if the force level of 17 MN exceeds substantially the maximum resistance to penetration of a rigid brace, i.e. 12.5 MN. This illustrates the importance of interaction; the stern resistance to penetration by a dented brace is larger than that of a rigid brace. The same behavior is experienced for a thickness of 40 mm, but ultimately, for a force level 16 MN, the brace starts to penetrate the ship. However, the brace has

been pushed significantly into the tensile membrane action, and brace fracture due to excessive straining may take place. The stern's resistance to penetration continues to drop for 50 mm brace thickness, but significant brace denting and beam deformation take place. Evidently, the brace collapse resistance (R_0 = *13.2* MN) is not sufficient to avoid extensive brace damage. Only when the thickness is increased to 60 mm, with a collapse resistance of R_0 *=15.9* MN, neither local denting nor beam deformation occur. Thus, the transition to strength design takes place around 55-60 mm brace wall thickness for this brace configuration. Similar observations are found for the stern end 1 collision with the 2.0m diameter tube in Fig. 32.

The brace response for stern end 2 impacts is similar, see Fig. 33. The contact width is much larger for this vessel, so the stern's resistance to penetration increases, but this is also the case for the brace plastic mechanism resistance. For wall thicknesses up to 50 mm, the brace undergoes extensive denting, but with 60 mm thickness, the brace is capable of penetrating the stern without local denting and beam bending. The corresponding R_0 = *20.4* MN is close to the stern's resistance to penetration. Again, for this brace configuration the transition to strength design takes place for brace wall thickness of 55-60 mm with the corresponding $R_c \sim$ *1.12-1.28* MN; In addition, the bending resistance, R_0, accounting for the contact height, should exceed the stern's resistance to penetration.

The required R_c values for different stern end collision scenarios are summarized in Table 8. The considerations and conclusions are quite similar with stern corner collision cases. From Table 8, an R_c value of 1.5 MN is recommended for braces/legs to maintain compactness in stern end collisions, which is conservative.

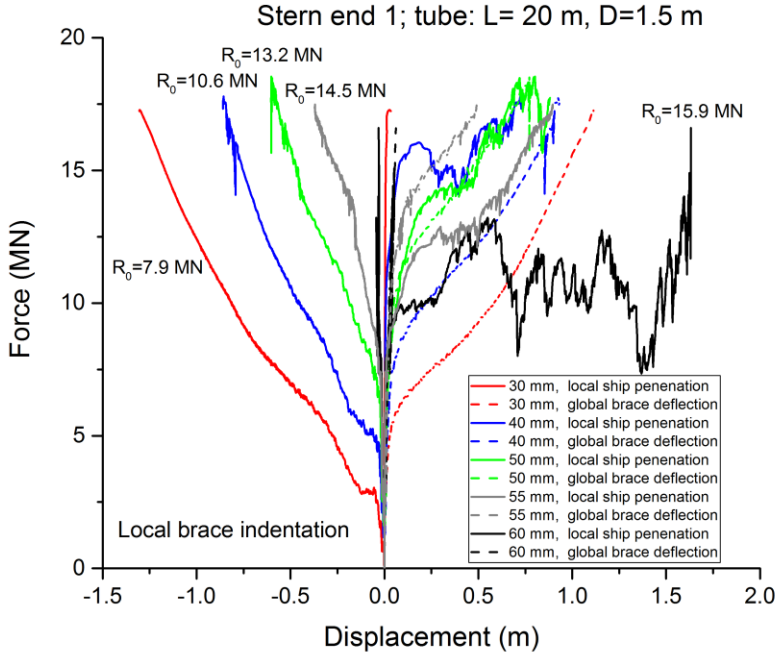

Fig. 31. Force versus local indentation and beam deformation of brace and force-versus penetration of stern end 1 - vertical brace with 1.5m diameter and varying thicknesses

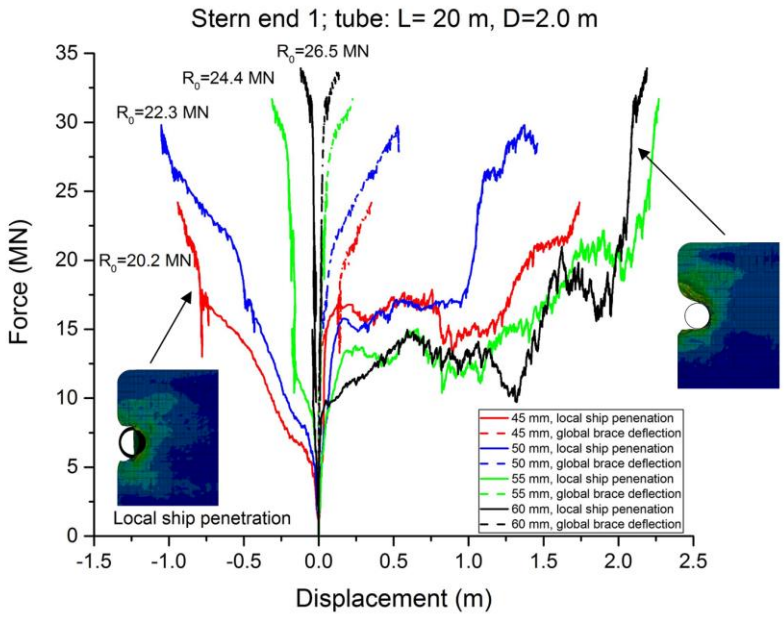

Fig. 32 Force versus local indentation and beam deformation of brace and force-versus penetration of stern end 1 - vertical brace with 2.0 m diameter and varying thicknesses

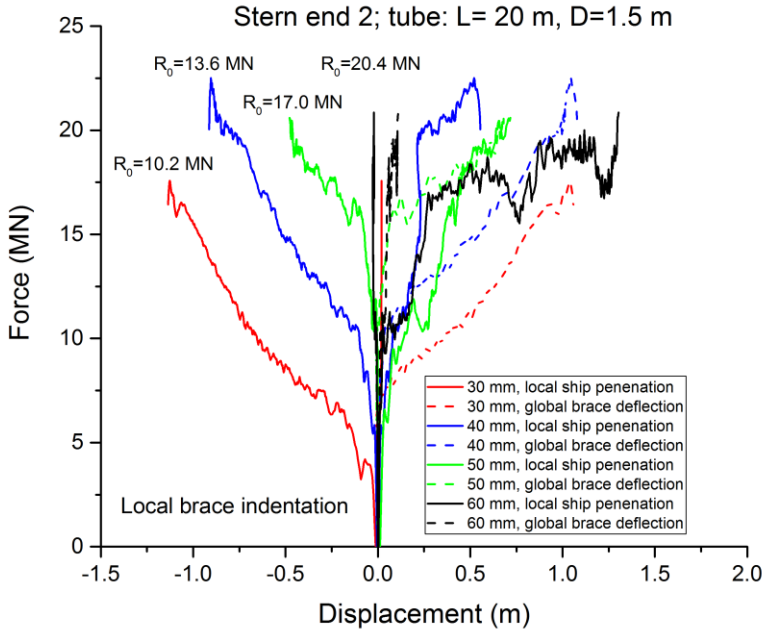

Fig. 33 Force versus local indentation and beam deformation of brace and force-versus penetration of stern end 2 - vertical brace with 1.5m diameter and varying thicknesses

Table 8. The required R_c values for different stern end collision scenarios

Striking ship	*Brace dimension L(m) × D(m)*	*The required tube thickness t (mm)*	*Corresponding R_c (MN)*	*Corresponding R_0 (MN)*
Stern end 1	20×1.5	60	1.28	14.6
Stern end 1	20×1.5 (battered leg)	60	1.28	14.6
Stern end 1	20×2.0	60	1.48	26.5
Stern end 2	20×1.5	60	1.28	18.8
Stern end 2	20×2.0	60	1.48	34.1
Stern end 2	15×2.0	55	1.30	47.0
Stern end 2	25×2.0	60	1.48	25.6

8. Conclusions

The current DNV-GL design standards for ships and offshore structures against accidental ship impacts were developed more than 30 years ago. Over these years, significant changes of the supply vessels have taken place, notably increasing size and new structural configurations (bulbous bows, X-bows, etc). This has triggered the need for revision of recommended practices for ship collisions design, and a new version DNV-GL RP C204 is under preparation.

A large number of nonlinear finite element simulations were carried out with LS-DYNA for jacket braces/legs impacted by a bulbous bow and two stern corners/ends of modern supply vessels. Both the braces/legs and the ship were modeled with shell finite elements, thus allowing important interaction effects to be studied in detail. Several numerical simulations demonstrated that the ship resistance to penetration increases if the brace/leg is subjected to local denting. This will be accounted for in the updated DNV-GL RP C204.

Numerical analysis with deformable ship and rigid braces showed that the force level in the current design force-displacement curves should be increased to account for larger, modern supply vessels.

As the design collision energy in the revised NORSOK N-003 standard increases significantly to 50 MJ for bow impacts and 22 MJ for stern impacts, it is virtually impossible for braces/legs to absorb the entire energy (i.e. ductile design). Hence, it may be necessary to aim for strength design or shared energy design; i.e. the brace/leg should be capable of penetrating substantially into the ship structure.

To obtain sufficient plastic mechanism resistance of braces/legs, local indentations should be minimized by satisfying the denting compactness criterion. Existing denting resistance models and compactness criteria were reviewed. The Wierzbicki and Suh [10] resistance model was extended to consider distributed loads, and the modified resistance versus local denting relationships agreed well with the results of numerical simulations.

The concept of ‘transition indentation ratio’, $w_{d,tran}/D$, for braces and legs where the deformation switches from local denting to plastic bending was discussed. The transition ratio shows which deformation pattern (local denting or global bending) is dominant for braces and legs with certain

dimensions and material properties. It was found that several compactness criteria in the literature were essentially similar, which limited the transition ratio. It was found, however, that with small transition ratios, local denting may still continue in the global bending stage. Hence, it is suggested to use R_c as the compactness requirement, following the recommendations by Storheim and Amdahl [22]. Based on numerical simulation results, R_c is suggested to be 1.2 MN for stern corner impacts, and 1.5 MN for stern end impacts. For bow collisions with horizontal and diagonal braces, $R_c = 1.9 F_{max}/24$, where F_{max} is the maximum collision force.

Acknowledgments

This work has been funded by the Research Council of Norway (NFR) through the Centers of Excellence funding scheme, project AMOS (Grant number 223254) at the Norwegian University of Science and Technology (NTNU). This support is gratefully acknowledged by the authors.

References

[1] DNV. Impact loads from boats. Technical Note for Fixed Offshore Installations TN A. 1981;202.
[2] Kvitrud A. Collisions between platforms and ships in Norway in the period 2001-2010. ASME 2011 30th International Conference on Ocean, Offshore and Arctic Engineering: American Society of Mechanical Engineers; 2011. p. 637-41.
[3] DNV. NORSOK Standard N004. Design of steel structures, Appendix A, design against accidental actions. Det Norske Veritas 2004. 2004.
[4] DNV-RP-C204. Recommended practice DNV-RP-C204. DET NORSKE VERITAS. 2010.
[5] Yu Z, Shen Y, Amdahl J, Greco M. Implementation of Linear Potential-Flow Theory in the 6DOF Coupled Simulation of Ship Collision and Grounding Accidents. J Ship Res. 2016;60:119-44.
[6] Yu Z, Amdahl J, Storheim M. A new approach for coupling external dynamics and internal mechanics in ship collisions. Marine Structures. 2016;45:110-32.
[7] Yu Z, Amdahl J. Full six degrees of freedom coupled dynamic simulation of ship collision and grounding accidents. Marine Structures. 2016;47:1-22.
[8] Furnes O, Amdahl J. Ship collisions with offshore platforms. Intermaritec'80. 1980.
[9] Amdahl J. Impact Capacity of Steel Platforms and Tests on Large Deformations of Tubes and Transverse Loading. Det norske Veritas, Progress Report. 1980:80-0036.
[10] Wierzbicki T, Suh M. Indentation of tubes under combined loading. International Journal of Mechanical Sciences. 1988;30:229-48.
[11] Soares CG, Søreide TH. Plastic analysis of laterally loaded circular tubes. Journal of Structural Engineering. 1983;109:451-67.
[12] Ellinas CP, Walker AC. Damage on offshore tubular bracing members. IABSE Colloquium on Ship Collisions With Bridges and Offshore Structures, Copenhagen, May1983. p. 253-61.
[13] Jones N, Shen W. A theoretical study of the lateral impact of fully clamped pipelines. Proceedings of the Institution of Mechanical Engineers, Part E: Journal of Process Mechanical Engineering. 1992;206:129-46.
[14] Buldgen L, Le Sourne H, Pire T. Extension of the super-elements method to the analysis of a jacket impacted by a ship. Marine Structures. 2014;38:44-71.
[15] Amdahl J. Energy absorption in ship-platform impacts. Doctoral Thesis, Norwegian Institute of technology1983.
[16] Jones N, Birch S, Birch R, Zhu L, Brown M. An experimental study on the lateral impact of fully clamped mild steel pipes. Proceedings of the Institution of Mechanical Engineers, Part E: Journal of Process Mechanical Engineering. 1992;206:111-27.

[17] Sherman DR. Test of circular steel tubes in bending. Journal of the Structural Division. 1976;102:2181-95.
[18] Norsok. Actions and action effects, N-003. Oslo: Norwegian Technology Standards Institution. 2017.
[19] Amdahl J, Johansen A. High-energy ship collision with jacket legs. The Eleventh International Offshore and Polar Engineering Conference: International Society of Offshore and Polar Engineers; 2001.
[20] Cho SR. Design approximations for offshore tubulars against collisions. PhD Thesis, Glasgow University, UK. 1987.
[21] RP2A-WSD A. Recommended practice for planning, designing and constructing fixed offshore platforms–working stress design–. Twenty-2000.
[22] Storheim M, Amdahl J. Design of offshore structures against accidental ship collisions. Marine Structures. 2014;37:135-72.
[23] Cerik BC, Shin HK, Cho S-R. A comparative study on damage assessment of tubular members subjected to mass impact. Marine Structures. 2016;46:1-29.
[24] Tørnqvist R. Design of crashworthy ship structures: Technical University of Denmark Kgns Lyngby,, Denmark; 2003.
[25] de Oliveira J, Wierzbicki T, Abramowicz W, Veritas N. Plastic Behaviour of Tubular Members Under Lateral Concentrated Loading: Det norske Veritas, Research Division; 1982.
[26] DNV-RP-C208. Determination of Structural Capacity by Non-linear FE analysis Methods. Det Norske Veritas. 2016.

Appendix: structural details of the bow and sterns analyzed

The joint industry project that established the DNV RP C208 prepared the structural models of modern offshore supply vessels (OSV) for ship collision analysis. The models are available for downloads from the link given in the appendix A of the revised DNV RP C208 [26]. The revised version of DNV RP C208 can be downloaded from the following link:

https://rules.dnvgl.com/docs/pdf/DNVGL/RP/2016-09/DNVGL-RP-C208.pdf?utm_campaign=&utm_medium=email&utm_source=Eloqua

The structural models are briefly introduced.

1. The ship bow model

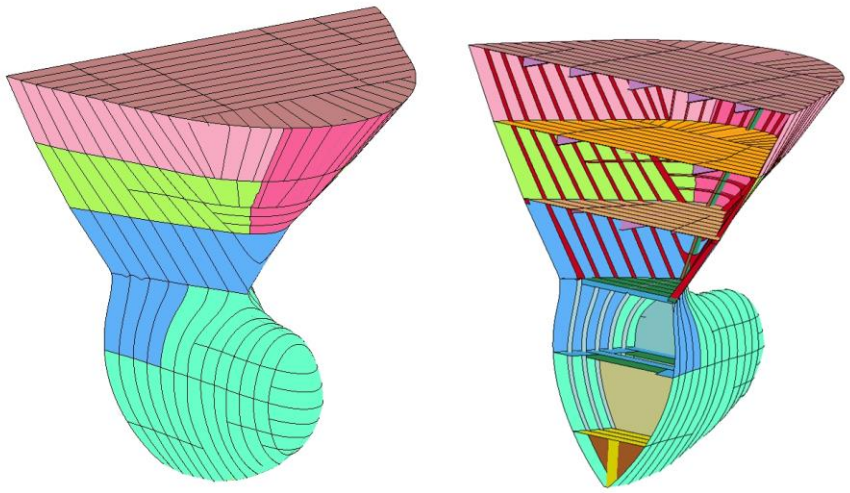

Fig. A1. The ship bow model

General dimensions

Displacement	7500 tons
Length	91 m
Breadth	18.8 m
Depth	7.6 m
Draft	6.2 m

Scantlings of structural components

Bulb second deck plate thickness	9 mm
Bulb bulkhead plate thickness	9 mm
Bulb longitudinal frame plate thickness	10.5 mm
Bulb transverse frame plate thickness	9.5 mm
Bulb breast hook plate thickness	12 or 15 mm
Bulb ring stiffeners	Flat Bar 250 mm*15 mm, spacing 600 mm

Forecastle, 1st and 2nd deck, plate thickness	8 mm
Deck stiffeners	Flat Bar, web 160 mm (height) *11.6mm (thickness), length varies with location, spacing 0.6 m.
Deck girder	T type, web 385mm*10 mm, flange 150 mm*9 mm, length varies with location, spacing 2.35m
Stem hull plate thickness	Upper 9 mm, middle 11 mm, lower 12.8mm
Bulb plate thickness	12.5 mm

2. The model of stern 1

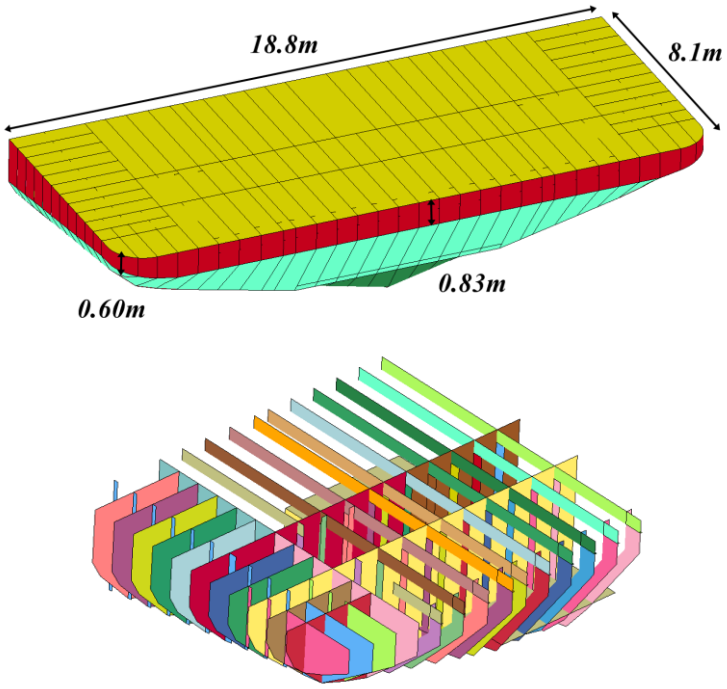

Fig. A2. The ship stern 1 model

General dimensions

The stern 1 model and the bow model are from the same supply vessel.

Scantlings of structural components

Outer bottom plate thickness	11 mm
Inner bottom plate thickness	15 mm
Deck plate thickness	15 mm
Transverse frame	Thickness 10 mm, spacing 0.65 m
Longitudinal frame	Thickness 15 mm, spacing 0.65 m

Longitudinal stiffeners	L8.1m*0.32m*0.05m*12 mm, spacing 0.65 m
Side shell thickness	Lower 11 mm, upper 20 mm

3. *The model of Stern 2*

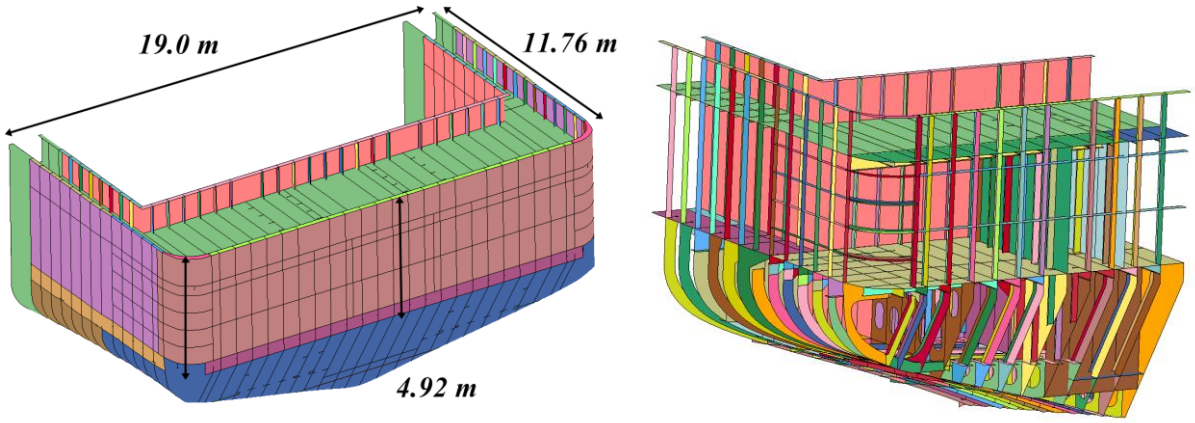

Fig. A3. The ship stern 2 model

General dimensions

Displacement	7500 tons
Draft	6.2 m

Scantlings of structural components

The stern 2 model is very complex with more than 500 parts in LS-DYNA. Only scantlings of the main structural components are described.

Outer hull plate thickness	11 or 12 mm
Hull plate stiffeners	L 4430*190*38*15 mm, spacing 0.7m
Deck plate thickness	14 mm
Transverse frame	Thickness 9 mm, spacing 0.7 m
Longitudinal frame	Thickness 12 mm, spacing 0.7 m